Island arc tholeiites of Early Silurian, Late Jurassic and Late Cretaceous ages in the El Fuerte region, northwestern Mexico

Ricardo Vega-Granillo*, Jesús Roberto Vidal-Solano, and Saúl Herrera-Urbina

Departamento de Geología, Universidad de Sonora, Rosales y Encinas s/n, 83000 Hermosillo, Sonora, México.
**rvega@ciencias.uson.mx*

ABSTRACT

Three distinctive igneous suites crop out in the El Fuerte block, northwestern Mexico. The oldest of these suites is the Realito Gabbro, which intrudes the Middle-Upper Ordovician Río Fuerte Formation. This gabbro yielded an Early Silurian U-Pb zircon age of ca. 430 ± 15 Ma. The Topaco Formation is a greenschist facies metamorphosed volcanosedimentary sequence. Basaltic rocks of this unit yielded a Late Jurassic U-Pb zircon age of 155 ± 3.5 Ma (Kimmeridgian). The Guamuchil Formation mainly consists of basaltic flows overprinted by greenschist facies contact metamorphism. A sample of this unit yielded a Late Cretaceous U-Pb zircon age of 73 ± 1.5 Ma (Campanian). Geochemical signatures of the three suites suggest an island arc tholeiitic environment. The Upper Jurassic Cubampo Granite is a peraluminous subalkaline granite. Age coincidence and similarities in rare earth element patterns and trace elements concentrations suggest that a genetic link exists between the Cubampo Granite and the Topaco Formation. In a regional context, the Realito Gabbro is coeval with Silurian rocks of the Acatlán Complex in southern Mexico, although geochemical data indicate they originated in different tectonic settings. In a larger scale, the Realito Gabbro rocks are coeval with rocks located along the Appalachian chain and northwestern South America. Late Jurassic magmatism in the El Fuerte region may be the southern prolongation of the continental magmatic belt of Sonora and southwestern USA. Late Cretaceous magmatism of the Guamuchil Formation may correlate with the Sonora-Sinaloa belt of intrusive and volcanic rocks, which was emplaced after accretion of the Guerrero terrane. The island arc tectonic setting indicated by geochemistry of the Mesozoic suites in the El Fuerte region differs from the continental arc setting of north-central Sonora and southwestern USA, which is probably due to mantle source differences.

Key words: island arc magmatism, Early Silurian, Late Jurassic, Late Cretaceous, El Fuerte, Sonobari, Sinaloa, Mexico.

RESUMEN

En el bloque El Fuerte, situado al norte del estado de Sinaloa en el noroeste de México, afloran tres grupos ígneos distintivos. La unidad más antigua es el Gabro Realito, el cual intrusiona a la Formación Río Fuerte del Ordovícico Medio-Superior. Este gabro produjo una edad U-Pb en zircones de ca. 430 ± 15 Ma, correspondiente al Silúrico Temprano. La Formación Topaco es una secuencia volcanosedimentaria con metamorfismo en facies de esquisto verde. Análisis U-Pb en zircones separados

Vega-Granillo, R., Vidal-Solano, J.R., Herrera-Urbina, S., 2012, Island arc tholeiites of Early Silurian, Late Jurassic and Late Cretaceous ages in the El Fuerte region, northwestern Mexico: Revista Mexicana de Ciencias Geológicas, v. 29, núm. 2, p. 492-513.

de una roca basáltica de esta unidad produjo una edad de 155 ± 3.5 Ma (Kimmeridgiano). La Formación Guamúchil está formada principalmente por flujos basálticos con un metamorfismo de contacto en facies de esquisto verde. En una muestra de esta unidad se obtuvo un edad U-Pb en zircones de 73 ± 1.5 Ma (Campaniano). La firma geoquímica de los tres grupos es muy similar e indica que corresponden a toleítas de arco de islas. Las características geoquímicas del Granito Cubampo del Jurásico Superior y rocas relacionadas, indica que se trata de un granito subalcalino peraluminoso. Similitudes en las concentraciones de elementos de las tierras raras y otros elementos traza entre el Granito Cubampo y las rocas máficas de la Formación Topaco sugieren algún tipo de relación genética entre ambas unidades. En un contexto regional, el Gabro Realito es contemporáneo de las rocas silúricas del Complejo Acatlán que afloran en el sur de México, aunque diferencias geoquímicas y en las condiciones de metamorfismo indican que los contextos tectónicos para ambas regiones fueron diferentes. En una escala mayor, el Gabro Realito es contemporáneo de rocas localizadas a lo largo de la cadena apalachiana o en el noroeste de América del Sur. Considerando su edad, el magmatismo del Jurásico Tardío en la región de El Fuerte puede corresponder con la prolongación al sur de un cinturón magmático continental que se extiende a través de Sonora desde el suroeste de los EUA, o bien, puede corresponder al magmatismo del Jurásico Tardío-Cretácico Temprano del terreno compuesto Guerrero. El magmatismo del Cretácico Tardío de la Formación Guamúchil puede relacionarse al cinturón magmático de Sonora-Sinaloa, formado por rocas intrusivas y volcánicas emplazadas después de la acreción del terreno Guerrero. El contexto tectónico de arco de islas indicado por la geoquímica de las rocas mesozoicas en la región de El Fuerte difiere del contexto de arco continental de Sonora central-norte y suroeste de los EUA, lo cual se considera producido por diferencias en la fuente mantélica.

Palabras clave: magmatismo de arco insular, Silúrico Temprano, Jurásico Tardío, Cretácico Tardío, El Fuerte, Sonobari, Sinaloa, México.

INTRODUCTION

The El Fuerte block consists of metamorphic rocks that crop out in northern Sinaloa, about 300 km south of the Laurentian craton boundary (Figure 1). This block is a piece of a late Paleozoic orogen located outboard of the Sonora-Marathon-Ouachita fold-and-thrust belt (Poole *et al.*, 2005). That location suggested an exotic origin that contrasts with the Laurentian blocks of central and northern Sonora (Poole *et al.,* 2005). The basement of the El Fuerte block is the Sonobari complex (de Cserna and Kent, 1961; Campa and Coney, 1983). This complex is comprised by the Middle to Upper Ordovician Río Fuerte Formation (Mullan, 1978; Poole *et al.*, 2005; Vega-Granillo *et al.*, 2008) and the Late Jurassic Topaco Formation (Vega-Granillo *et al.*, 2008), which crop out east of the El Fuerte town, as well as the Late Triassic (?) Francisco Gneiss (Mullan, 1978; Anderson and Schmidt, 1983; Keppie *et al.,* 2006) which crops out west of the El Fuerte town. Detrital zircon data from the Río Fuerte Formation indicate a peri-Gondwanan provenance (Vega-Granillo *et al.*, 2008). The terranes map of Campa and Coney (1983) shows that the Sonobari Complex is surrounded by the Guerrero Terrane or superterrane (inset in Figure 1). This terrane is composed by Upper Jurassic to Lower Cretaceous volcanic, volcanosedimentary and minor sedimentary rocks (Campa and Coney, 1983), deposited over a Late Triassic metamorphosed basement (Centeno-García *et al.,* 1993).

This study deals with three igneous units cropping out in the El Fuerte area, which lack detailed geochemical or isotopic studies. Tentative ages of Late Cretaceous, Late Jurassic, and Early Cretaceous, were previously proposed by Mullan (1978) for the Realito Gabbro, Topaco Formation and Guamuchil Formation, respectively, based on petrology, geological relationships, and correlations. In this work, we present a U-Pb geochronology study, aimed to obtain precise ages. Additionally, geochemical analyses of major, minor, and rare earth elements, were performed on selected rocks of each unit to identify their geochemical affinity and tectonic setting. Based on these data, a list of the igneous units that may correlate with those of the study area is included, and the probable associated tectonic scenarios are discussed.

ANALYTICAL METHODS

U-Pb isotopic ratios of zircons were measured by laser ablation multicollector inductively coupled plasma mass spectrometry (LA-MC-ICPMS) at the University of Arizona LaserChron Center using the procedures described by Gehrels *et al.* (2006).

Mineral composition was determined using a CAMECA SX-100 electron microprobe at the Department of Lunar and Planetary Sciences of the University of Arizona. For the geochemical measurements in whole rock, samples were ground first in a steel jaw crusher and then finely powdered in an agate grinder. Major and compatible trace elements were quantified by inductively coupled plasma atomic emission spectrometry (ICP-AES), whereas rare earth elements (REE) and additional trace elements were obtained for a subset of samples by inductively coupled plasma-mass spectrometry (ICP-MS) at ALS

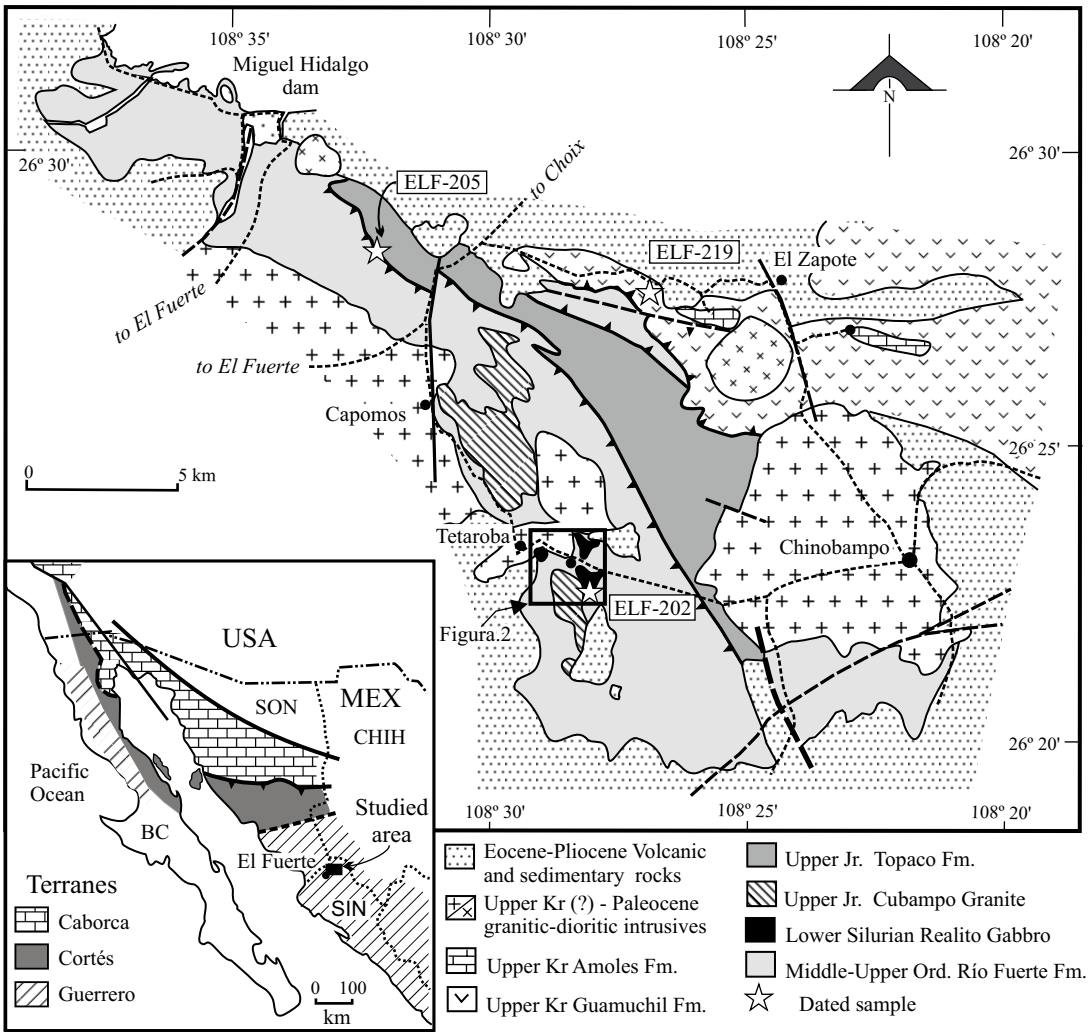

Figure 1. Geological map of the El Fuerte region (modified from Mullan, 1978). Inset: Map of the main terranes of northwestern Mexico (adapted from Poole *et al.*, 2005). BC: Baja California; CHIH: Chihuahua; SIN: Sinaloa; SON: Sonora. Stars indicate the location of dated samples.

Chemex laboratory. Some major element compositions were obtained using a Bruker SRS3400 WD-XRF spectrometer at the "Laboratorio de Cristalografía y Geoquímica del Departamento de Geología" of the Universidad de Sonora. Analytical errors are 1–3% for major elements and about 3% for trace elements.

GEOLOGICAL SETTING

The Río Fuerte Formation is the oldest unit in the study area (Figure 2). This unit consists of greenschist to amphibolite metasedimentary rocks (Vega-Granillo *et al.*, 2011) containing Middle to Late Ordovician conodonts (Poole *et al.*, 2005). Detrital zircons data indicate deposition in an intra-oceanic basin located between an Ordovician arc and an extinct peri-Gondwanan arc (Vega-Granillo *et al.*, 2008). The Río Fuerte Formation underwent at least two low P/T (Buchan type) metamorphic events, which are coeval with two deformational phases (Vega-Granillo *et al.*, 2011).

The greenschist metamorphosed Cubampo Granite and related aplite sills intrude the Río Fuerte Formation yielding ages of 155 and 151 Ma, respectively (U-Pb, zircon; Vega-Granillo *et al.*, 2008). The Realito Gabbro, also intruding the Río Fuerte Formation (Figure 3), was tentatively considered as Late Cretaceous in age (Mullan, 1978), but a precise age is presented in this work.

The Topaco Formation is a greenschist metamorphosed volcanic and volcaniclastic unit assigned to the Late Jurassic (Mullan, 1978) on the basis of geological relationships. Meta-agglomerates of this unit contain clasts of the Upper Jurassic Cubampo aplite as well as clasts of the Río Fuerte Formation (Vega-Granillo *et al.*, 2011). The Río Fuerte Formation is thrust over the Topaco Formation. Although precise ages for metamorphic events in the El Fuerte units are unknown, the first event affecting only the Río Fuerte Formation must have occurred between the Late Ordovician and Late Jurassic times; and the second, imposed

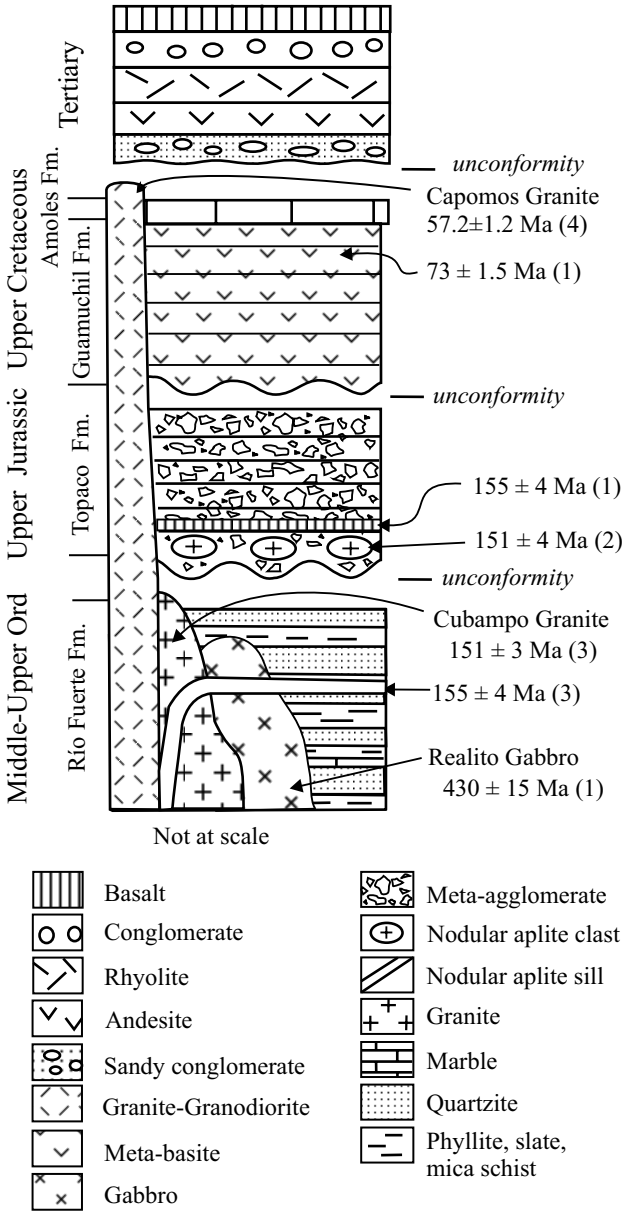

Figure 2. Schematic stratigraphic column of the El Fuerte region. U-Pb zircon ages: 1) this work; 2) Vega-Granillo *et al.* (2008); 3) Vega-Granillo *et al.* (2011); 4) K-Ar biotite age Damon *et al.* (1983).

on both, the Río Fuerte and Topaco formations, may be Late Jurassic in age (Vega-Granillo *et al.,* 2008).

The Guamuchil Formation is a thick unit made of lava flows with greenschist facies contact metamorphism, which structurally overlies the Río Fuerte and Topaco formations. In turn, this unit is overlain by ~100 m of slightly recrystallized micritic limestones named Los Amoles Formation (Mullan, 1978), in which no fossils have been founded. In spite of lacking fossils, limestones of this unit were tentatively correlated with fossiliferous Albian-Cenomanian beds of the Alisitos Formation from Baja California (Mullan, 1978). Based on that correlation, the Guamuchil Formation was considered as the volcanic lower section of the Alisitos Formation, and consequently, of Early Cretaceous age (Mullan, 1978). However, a precise age for the Guamuchil Formation is included in this work. Granodioritic to dioritic bodies referred to as the Capomos Granite intrudes all previous units. These intrusives yielded K-Ar biotite ages of 57.2 ± 1.2 Ma (Damon *et al.*, 1983).

Lithological units

Realito Gabbro

This unit includes three small gabbro intrusions (<1 km wide) outcropping near the town of Realito (Figure 3). Mafic dikes crosscut the gabbro and are regarded as part of the same suite by their close field relationship. The gabbro plutons intrude the Río Fuerte Formation and, in turn, both units are intruded by the Upper Jurassic Cubampo Granite and the Paleocene Capomos Granite (Figure 1).

The Realito Gabbro is composed of large amphibole crystals containing anhedral relics of Al-Cr diopside. Amphibole and pyroxene classification diagrams are included in Figure 4. Metamorphic minerals partially replaced the gabbro original mineralogy during regional and/or contact metamorphism events; in particular, plagioclase is absent due to total replacement by secondary minerals. Secondary fine-grained clinozoisite-epidote, chlorite, and actinolite, surround large amphibole crystals. Amphibole zoning is complex including Mg-hornblende cores with Mg-hastingsite and pargasite rims, which in turn, are irregularly replaced by zones of actinolite and minor tremolite.

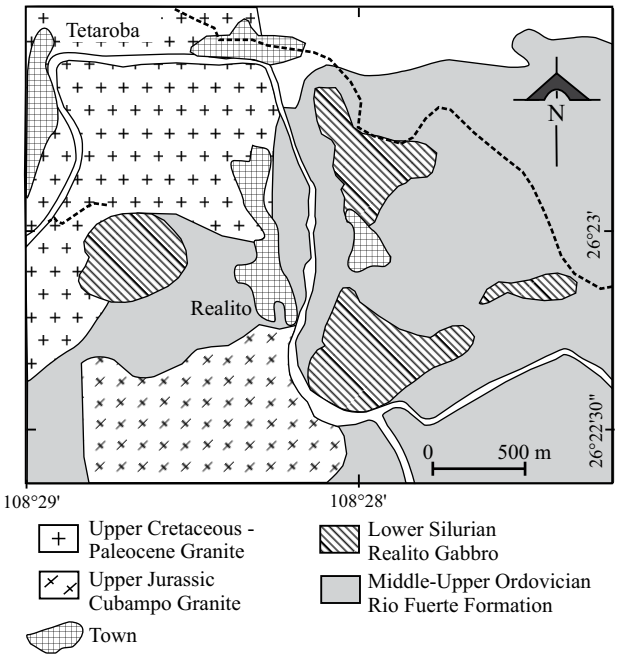

Figure 3. Detailed geological map of the Realito Gabbro intrusion.

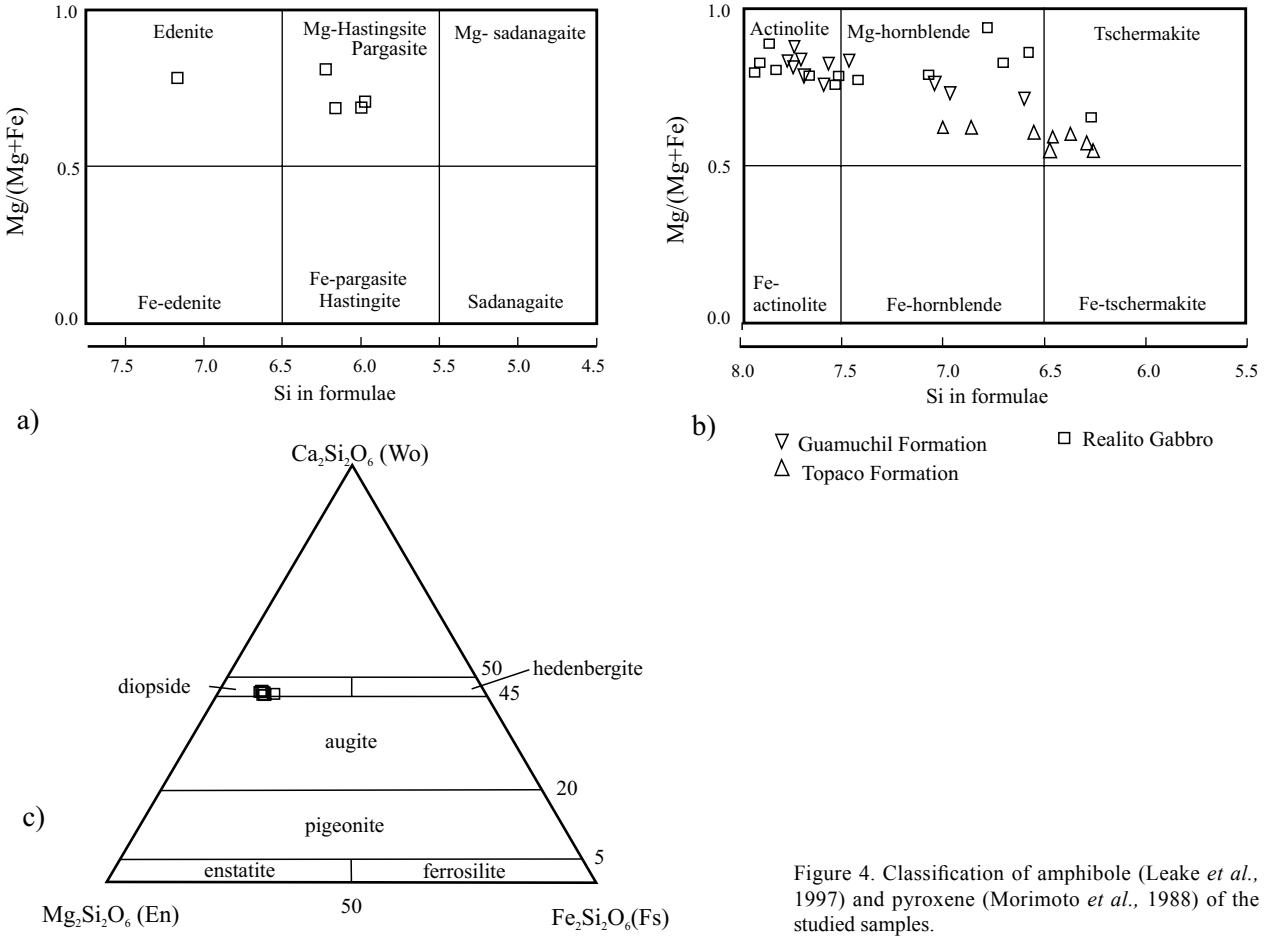

Figure 4. Classification of amphibole (Leake *et al.,* 1997) and pyroxene (Morimoto *et al.,* 1988) of the studied samples.

Mafic dikes cutting the gabbro display an incipient foliation and are made of fibroradial amphibole and labradorite, with secondary zoisite, chlorite, titanite, and calcite. Thin veinlets of quartz + chlorite + calcite + epidote crosscut the gabbro and dikes.

Cubampo Granite

This unit includes an irregular shaped granite stock, aplitic dikes and sills, as well as isolated enclaves of medium-grey color. These rocks intrude the Río Fuerte Formation and the Realito Gabbro (Figures 1 and 3). Aplite sills emplaced along the Middle to Upper Ordovician Río Fuerte metasedimentary rocks were originally considered as a rhyolite flow and used as stratigraphic marker (Mullan, 1978); however, a sill yielded a 155 ± 4 Ma age confirming its intrusive character (Vega-Granillo *et al.*, 2008). The main Cubampo body and related sills are characterized by nodules of quartz as large as 1.5 cm. Mineralogy consists of K-feldspar, quartz, plagioclase, and minor muscovite, biotite, titanite and zircon. Retrogressive metamorphic minerals are epidote-zoisite, chlorite, tremolite, and sericite. Foliation is incipient in the main granitic body and more developed in the fine-grained aplite sills, occurring as aligned chlorite-sericite-epidote grains.

Topaco Formation

This unit mostly consists of meta-agglomerates, some intercalated metabasites, scarce metarhyolite, slate, quartzite, and minor mafic dikes, with a structural thickness varying from 1300 to 5000 m. Clasts in meta-agglomerates are petrographically similar to rocks of the Río Fuerte Formation and the Cubampo Granite. One nodular aplite clast from the meta-agglomerate yielded a 151 ± 1 Ma age (U-Pb zircon, Vega-Granillo *et al.*, 2011) coincident with the ages of the Cubampo Granite and related sills. The Topaco Formation displays mesoscopic well-developed pervasive foliation, which is parallel to the S2 foliation of the Río Fuerte Formation. Structural relationships indicate the Río Fuerte Formation is thrust over the Topaco Formation (Vega-Granillo *et al.*, 2011).

Two samples of the Topaco Formation were collected for geochemical and geochronological studies. Sample ELF-205 is a mafic flow made of plagioclase phenocrysts and amphibole clusters in a groundmass of fine-grained plagioclase, amphibole, with accessory biotite and titanite. Sample ELF-206 is a diorite dike crosscutting andesite meta-agglomerates. Diorite consists of prismatic phenocrysts of amphibole surrounded by plagioclase + quartz groundmass. Plagioclase displays zoning from labradorite

to andesine and some myrmekite overgrowths. Amphibole has Mg-hornblende cores and actinolite rims (Figure 4). Metamorphic minerals like actinolite, epidote, chlorite, white mica, and calcite, partially replaced primary minerals, occurring also as thin veinlets.

Guamuchil Formation

This unit consists of dark-green to black volcanic flows, minor agglomerate and tuff. Mafic rocks display porphyritic to glomeroporphyritic texture, with plagioclase phenocrysts in clusters or isolated, in a groundmass of amphibole + plagioclase. Some metabasites contain spheroidal clusters of coarse-grained amphibole. Amphibole is mainly tschermakite, with minor Mg-hornblende, and outer rims of tremolite (Figure 4). Plagioclase is zoned with bytownite cores and oligoclase rims. Groundmass is made of secondary biotite + epidote + titanite + quartz. Mesoscopic lenses and layers of pale-green epidote, amphibole, quartz, chlorite and opaque minerals, are originated by hydrothermal metamorphism. Veinlets and lenses of amphibole ± quartz ± opaque minerals are common. Intermediate flows interbedded with metabasite consist of andesine phenocrysts in a groundmass of plagioclase + Kfeldspar + quartz + biotite (*e.g.*, ELF-214). Some of these rocks display a poorly developed foliation.

GEOCHRONOLOGY

Mafic rocks of the Realito Gabbro, Topaco and Guamuchil formations were sampled for U-Pb zircon geochronology (Table 1, Figure 5), location of samples is included in Table 2. Sample ELF-202 from the Realito Gabbro is a coarse-grained hornblende-pyroxene gabbro. Very few zircons obtained from this sample are light pink in color, with euhedral to subhedral shape. Four zircons yielded a mean weighted age of 430 ± 15 Ma (Llandovery) with a MSWD of 0.6 (Figure 5a). Dated zircons have Th/U ratios from 0.5 to 2.3 suggesting a magmatic origin, provided that metamorphic zircons usually have Th/U ratios <0.07 (Rubatto, 2002). Five younger ages varying from Mississippian to Late Cretaceous are mostly isolated and are considered as produced by Pb-loss related with later metamorphic events, although one Late Jurassic (156 Ma) and one Early Cretaceous (144 Ma) ages are also concordant.

In the Topaco Formation sample (ELF-205), six light pink, euhedral to subhedral zircons making the only cluster of the sample yielded a mean weighted age of 155 ± 3.5 Ma age (Kimmeridgian) with a MSWD of 1.3 (Figure 5b). Besides these six zircons, only one inherited Precambrian zircon was dated. Because no younger ages were obtained and Th/U ratios vary from 0.26 to 0.61, the Late Jurassic age is considered representative of the magmatic age of the sample.

The Guamuchil Formation dated sample (ELF-219) is a fine-grained mafic rock made up of amphibole and plagioclase, with pseudomorph lenses of zeolite + chlorite ± amphibole. Fourteen dated zircons yielded an age of 73 ± 1.5 Ma (Campanian) with a MSWD of 1.5 (Figure 5c), interpreted as indicating its magmatic crystallization. Older ages are considered as coming from inherited zircons.

GEOCHEMISTRY

Major and trace element compositions of all dated igneous units from the El Fuerte area were obtained (Table 3) and its location included in Table 2. Major element compositions were normalized to 100% on a volatile-free basis before being plotted. Some altered rocks were studied to see how metamorphism might have modified their geochemical composition; anyway, most rocks display coherent distribution of major elements and therefore, metamorphism is assumed to be mostly isochemical.

The Realito Gabbro has a subalkaline character with low TiO_2 (<0.7 wt.%), low SiO_2 and low alkalis contents (Figure 6a). The low ratios of the high field strength (HFS) elements Nb/Y and Zr/Ti (Figure 6b), which are generally immobile (Rollinson, 1993) confirm this feature. High FeOt concentration shows a typical tholeiitic signature (Figure 7a and 7b). The gabbro is characterized by its high content of MgO (~18 wt.%), Ni, Cr, and Co.

Fine-grained mafic dikes cutting the Realito Gabbro have tholeiitic composition, higher Al_2O_3, but lower MgO, Ni, Cr and Co, than the host rock. ELF 225 sample is richer in SiO_2 and Zr than the coarse-grained gabbro, but remains in the gabbro field (Figure 6a and 6b). Rare earth element (REE) spectra normalized to chondritic values of Sun and McDonough (1989) and incompatible multi-element patterns normalized to MORB (Pearce, 1983) relate gabbro and its crosscutting dikes (Figure 8a and 8d). Both types of rock are slightly enriched in light rare earth elements (LREE) [$(La/Yb)_N$ = 3.40 – 4.25], and depleted in heavy rare earths elements (HREE). REE abundances are mostly lesser than 10X the chondritic relation. This feature distinguishes microgabbro dikes from rocks of the Topaco and Guamuchil formations (Figure 8a, 8c). MORB-normalized multi-element spectra of the Realito Gabbro and microgabbro display enrichment of low-field strength (LFS) elements and depletion of high-field strength (HFS) elements (Figure 8d). Their patterns are characterized by 1) forming a hump in Ce-P, and a more pronounced one in Rb, Ba and Th; and 2) slight negative anomalies in Nb. Gabbro and microgabbro normative composition includes plagioclase (Pl), olivine (Ol), diopside (Di), and hypersthene (Hy), which is distinctive of olivine tholeiites (Yoder and Tilley, 1962).

High content in MgO (~18%), Ni, Cr, and Co, in the Realito Gabbro suggests either a komatiitic affinity or derivation of a cumulate process. According to Seiferd *et al.* (1996) cumulate gabbros have lost most of the incompatible elements, which is specially obvious in the REE diagram, where they display REE abundance between 1X to 5X chondrite, while isotropic gabbros have abundances near

Table 1. U-Pb zircon geochronologic data.

Analysis	U (ppm)	$^{206}Pb/^{204}Pb$	U/Th	$^{206}Pb^*/^{207}Pb^*$	± (%)	$^{207}Pb^*/^{235}U^*$	± (%)	$^{206}Pb^*/^{238}U$	± (%)	Error corr	$^{206}Pb^*/^{238}U^*$	± (Ma)	$^{207}Pb^*/^{235}U$	± (Ma)	$^{206}Pb^*/^{207}Pb^*$	± (Ma)	Best age (Ma)	± (Ma)
ELF-202 Realito Gabbro																		
1	293	7170	2.0	17.2143	54.3	0.0292	54.6	0.0036	6.4	0.12	23.5	1.5	29.2	15.7	533.2	1283.0	23.5	1.5
2	1224	50421	1.2	20.5609	1.9	0.1516	2.3	0.0226	1.3	0.56	144.1	1.8	143.4	3.0	130.3	43.9	144.1	1.8
3	2374	47090	0.7	20.1498	0.8	0.1684	3.3	0.0246	3.2	0.97	156.7	5.0	158.0	4.9	177.6	18.6	156.7	5.0
4	5278	147957	0.3	20.2792	0.3	0.3850	11.0	0.0566	11.0	1.00	355.0	38.1	330.7	31.2	162.6	6.0	355.0	38.1
5	5314	49490	0.3	20.4047	0.2	0.3857	8.8	0.0571	8.8	1.00	357.8	30.7	331.2	24.9	148.2	5.8	357.8	30.7
6*	5268	57550	0.4	20.3018	0.4	0.4401	6.2	0.0648	6.2	1.00	404.8	24.2	370.3	19.2	160.1	9.3	404.8	24.2
7	84	20628	1.9	17.8695	9.2	0.5020	9.8	0.0651	3.5	0.35	406.3	13.7	413.1	33.4	450.8	204.8	406.3	13.7
8*	171	70876	1.7	18.0717	6.3	0.5052	6.4	0.0662	1.4	0.22	413.3	5.8	415.2	21.9	425.8	140.0	413.3	5.8
9*	346	6608	1.7	17.3902	3.0	0.5451	3.7	0.0687	2.3	0.61	428.6	9.5	441.8	13.4	510.9	65.0	428.6	9.5
10	171	18578	1.5	17.3353	5.3	0.5489	7.4	0.0690	5.2	0.70	430.2	21.6	444.3	26.6	517.8	116.1	430.2	21.6
11*	274	57574	2.1	18.1489	3.9	0.5380	5.2	0.0708	3.4	0.65	441.1	14.4	437.1	18.4	416.2	87.6	441.1	14.4
12	196	697801	2.5	9.1781	0.6	4.7707	1.9	0.3176	1.8	0.96	1777.8	28.2	1779.8	16.0	1782.0	10.2	1782.0	10.2
ELF-205 Topaco Formation																		
1*	671	51007	2.7	19.8069	3.2	0.1680	3.9	0.0241	2.3	0.59	153.8	3.5	157.7	5.7	217.5	73.0	153.8	3.5
2*	2149	116456	3.9	20.1289	0.9	0.1653	4.9	0.0241	4.9	0.98	153.7	7.4	155.3	7.1	180.0	22.1	153.7	7.4
3*	494	61750	2.3	20.1896	4.1	0.1696	4.3	0.0248	1.3	0.31	158.2	2.1	159.1	6.4	173.0	96.2	158.2	2.1
4*	654	25060	2.6	19.7429	3.8	0.1636	4.3	0.0234	2.1	0.48	149.3	3.1	153.8	6.2	225.0	87.7	149.3	3.1
5*	389	48806	2.8	21.0624	7.7	0.1673	9.8	0.0256	6.1	0.62	162.7	9.8	157.1	14.3	73.3	182.9	162.7	9.8
6	92	61585	1.6	11.1394	1.7	3.0415	2.3	0.2457	1.5	0.64	1416.4	18.5	1418.1	17.4	1420.7	33.3	1420.7	33.3
7*	162	7546	2.3	20.4143	27.0	0.1626	28.0	0.0241	7.6	0.27	153.3	11.5	152.9	39.8	147.2	642.7	153.3	11.5
ELF-219 Guamuchil Formation																		
1*	496	15511	1.4	20.6016	16.1	0.0737	17.3	0.0110	6.3	0.36	70.6	4.4	72.2	12.0	125.6	381.3	70.6	4.4
2*	4419	59459	221.8	20.9408	0.9	0.0717	3.8	0.0109	3.7	0.97	69.8	2.5	70.3	2.6	87.1	21.3	69.8	2.5
3*	1102	6661	111.2	20.2855	5.8	0.0789	6.3	0.0116	2.4	0.39	74.4	1.8	77.1	4.7	161.9	135.8	74.4	1.8
4*	2092	30224	47.1	20.7607	3.0	0.0766	3.6	0.0115	2.0	0.56	73.9	1.5	74.9	2.6	107.6	70.7	73.9	1.5
5	227	99092	1.1	10.9792	0.7	3.0710	3.0	0.2445	2.9	0.97	1410.2	36.9	1425.5	23.0	1448.3	14.1	1448.3	14.1
6*	1847	32262	60.2	20.8482	3.9	0.0783	4.4	0.0118	2.1	0.48	75.9	1.6	76.5	3.2	97.6	91.7	75.9	1.6
7	130	186836	1.6	12.5492	1.6	2.2562	2.8	0.2053	2.3	0.82	1204.0	25.4	1198.7	19.7	1189.3	31.5	1189.3	31.5
8*	1209	41372	33.6	20.8269	2.1	0.0778	2.5	0.0118	1.4	0.55	75.3	1.0	76.1	1.9	100.0	50.2	75.3	1.0
9*	1272	48860	35.2	20.6031	3.2	0.0817	8.9	0.0122	8.3	0.93	78.2	6.5	79.8	6.9	125.5	75.3	78.2	6.5
10	421	175872	2.0	15.9683	1.5	1.0036	3.3	0.1162	3.0	0.90	708.8	20.0	705.6	16.9	695.5	31.3	708.8	20.0
11	561	50700	3.4	16.2974	0.8	0.8723	3.0	0.1031	2.9	0.96	632.6	17.3	636.8	14.1	651.9	17.0	632.6	17.3
12	1138	32958	3.3	21.9135	7.3	0.0510	7.7	0.0081	2.6	0.34	52.1	1.4	50.5	3.8	-21.7	175.8	52.1	1.4
13	354	2623	19.3	21.8794	11.0	0.0803	12.2	0.0127	5.2	0.43	81.6	4.2	78.4	9.2	-17.9	266.5	81.6	4.2
14	427	20307	1.5	19.8156	15.1	0.0732	15.4	0.0105	3.1	0.20	67.5	2.1	71.8	10.7	216.5	351.9	67.5	2.1
15*	774	24865	3.5	21.8667	5.1	0.0700	6.5	0.0111	4.1	0.62	71.2	2.9	68.7	4.3	-16.5	123.4	71.2	2.9
16	5173	247444	19.1	20.9847	0.7	0.1355	6.7	0.0206	6.6	0.99	131.6	8.6	129.0	8.1	82.1	16.6	131.6	8.6
17*	1192	10730	1.4	19.3299	8.4	0.0796	9.5	0.0112	4.5	0.47	71.6	3.2	77.8	7.1	273.6	192.8	71.6	3.2
18*	936	28255	2.1	20.8456	7.0	0.0725	8.2	0.0110	4.2	0.52	70.3	3.0	71.1	5.6	97.9	165.4	70.3	3.0
19	218	11847	0.7	19.6419	14.0	0.1935	14.4	0.0276	3.4	0.24	175.3	5.9	179.6	23.7	236.8	324.4	175.3	5.9
20*	2971	84821	58.4	20.8847	1.7	0.0752	2.6	0.0114	1.9	0.75	73.0	1.4	73.6	1.8	93.4	39.8	73.0	1.4
21*	3907	6347	159.4	20.6463	2.1	0.0779	4.0	0.0117	3.3	0.85	74.8	2.5	76.2	2.9	120.6	49.5	74.8	2.5
22*	1443	45197	84.1	20.8075	3.1	0.0756	3.9	0.0114	2.3	0.59	73.1	1.7	74.0	2.8	102.2	74.4	73.1	1.7

* Data used to define age.

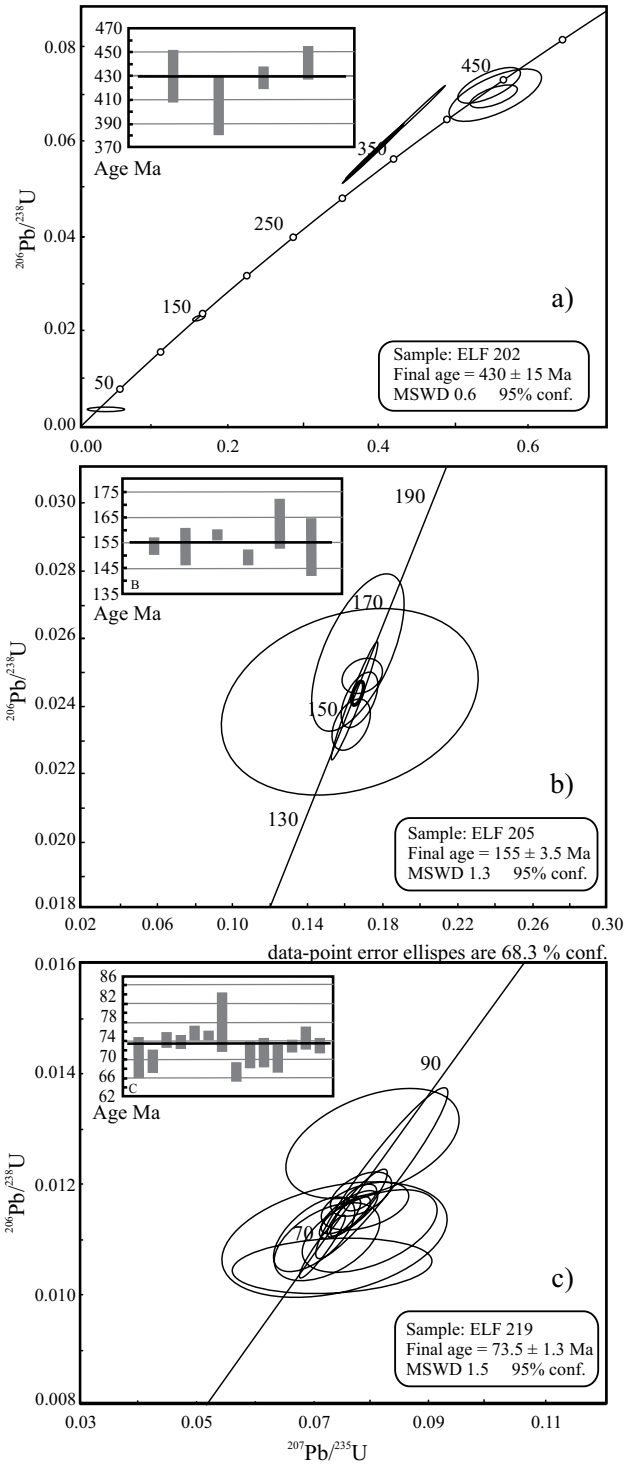

Figure 5. Concordia diagram and weighted-average ages of (a) Realito Gabbro; (b) Topaco Formation; (c) Guamuchil Formation.

or above 10X chondrite (Seiferd *et al.,* 1996). Both, the Realito gabbro and dikes have REE abundance lesser than 10X chondrite coinciding with those described for cumulate gabbros (Seiferd *et al.*, 1996). Although a cumulate origin can be proposed for the coarse-grained gabbro, this cannot be done for the dikes. An alternative explanation for the low REE abundances in both gabbro and microgabbro is a high degree of partial melting in the source (Best, 2003).

Table 2. Location of samples.

Sample	UTM coordinate (zone 12 R)	
ELF-200	750053	2922074
ELF-201	750083	2922086
ELF-202	752782	2919810
ELF-204	747307	2928560
ELF-205	745477	2929751
ELF-206	745897	2930744
ELF-207	750851	2930090
ELF-208	751247	2929960
ELF-209	752069	2929907
ELF-211	752613	2929820
ELF-214	754992	2929128
ELF-216	754373	2929565
ELF-217	753957	2929808
ELF-218	753902	2929839
ELF-219	753862	2929872
ELF-220	753507	2930156
ELF-221	753262	2920168
ELF-225	752910	2919855
ELF-226	751704	2920600

Cubampo Granite and related dikes correspond to peraluminous subalkaline granites with normative corundum (Figure 6a). Granites have high SiO_2 (75 – 78 wt.%) and Fe (2.2 – 3.4 wt.%) content. An enclave within the granite has quartzdiorite composition. All samples display a regular increase in LREE, a strong negative anomaly in Eu, and flat patterns for the HREE (Figure 8b) relative to chondrite. The aplite sample has a more depleted LREE and enriched HREE spectra. In the multi-element diagram, felsic rocks display spiky patterns due to: (1) a pronounced hump in Th and most large-ion lithophile (LIL) elements; (2) negative anomalies in Sr, P, and Ti; (3) much-less significant ones in Nb-Ta (Figure 8e).

The samples of the Topaco Formation, as those of the Realito Gabbro, have subalkaline mafic composition, tholeiitic affinity, similar concentration of REE [$(La/Yb)_N$ = 3.3–3.4], as well as low Ti and high Fe contents. Nevertheless, the Topaco Formation rocks have higher silica (52–53 wt.%) and alkalis (2.77–3.61 wt.%) content (Figure 6a). In addition, REE and multi-elements patterns are more enriched than those of the Realito Gabbro, although they are mostly parallel (Figure 8a, 8b, 8d and 8e). In addition, normative minerals in the Topaco Formation are quartz (Qtz), plagioclase (Pl), diopside (Di), and hypersthene (Hy), which is representative of quartz tholeiites (Yoder and Tilley, 1962). Similarities in REE and trace elements concentrations between Cubampo Granite rocks and mafic rocks of the Topaco Formation suggest some kind of genetic link between them, maybe peraluminous granites were formed

Table 3. Major (wt. %) and trace (ppm) element analyses of the El Fuerte metamorphic rocks.

	Realito Gabbro							Topaco Formation			
Sample n°	ELF-202*	ELF-202	ELF-221	ELF-225	ELF-226A	ELF-226B	ELF-226C	ELF-205*	ELF-205	ELF-206*	ELF-206
SiO_2 (wt %)	43.50	44.00	44.50	48.50	44.70	42.10	41.70	51.21	51.40	48.72	50.30
TiO_2	0.28	0.26	0.23	0.64	0.13	0.14	0.14	0.73	0.72	0.64	0.61
Al_2O_3	11.43	11.25	12.20	15.60	20.30	18.4	18.45	16.72	16.55	15.22	14.80
Fe_2O_3	11.14	10.90	8.96	10.35	7.01	9.55	10.15	9.85	9.68	8.90	8.40
MnO	0.19	0.20	0.16	0.33	0.13	0.16	0.17	0.18	0.18	0.16	0.15
MgO	17.03	17.50	17.10	7.38	9.67	10.10	10.60	5.76	5.76	7.96	7.84
CaO	11.43	10.80	10.35	10.70	13.90	13.90	13.10	10.85	10.20	8.48	7.84
Na_2O	0.03	0.42	0.36	2.61	0.71	0.45	0.43	1.74	2.20	2.58	3.06
K_2O	0.27	0.21	0.31	0.26	0.14	0.24	0.23	0.59	0.50	0.40	0.32
P_2O_5	0.07	0.06	0.08	0.21	0.02	0.02	0.02	0.21	0.20	0.11	0.11
LOI	4.32	4.32	4.37	1.9	1.88	3.85	4.06	2.30	2.30	6.61	6.61
Total	99.68	99.92	98.62	98.48	98.59	98.91	99.05	100.12	99.69	99.78	100.04
CIPW											
Q	0.00	0.00	0.00	0.00	0.00	0.00	0.00	6.36	5.55	1.12	2.09
or	1.65	1.29	1.92	1.61	0.82	1.48	1.42	3.62	3.06	2.54	2.01
ab	0.27	3.91	3.36	24.45	6.53	4.24	4.06	16.32	20.64	24.89	29.33
an	31.51	29.11	32.07	31.39	53.31	50.13	50.40	37.62	35.28	30.90	27.45
lc	0.00	0.00	0.00	0.00	0.00	0.00	0.00	0.00	0.00	0.00	0.00
ne	0.00	0.00	0.00	0.00	0.00	0.00	0.00	0.00	0.00	0.00	0.00
C	0.00	0.00	0.00	0.00	0.00	0.00	0.00	0.00	0.00	0.00	0.00
di	21.65	20.68	16.75	18.04	14.01	18.02	14.48	13.69	12.89	10.79	10.63
hy	19.10	16.54	24.30	16.32	12.30	3.58	5.15	18.50	18.70	26.25	25.09
ol	23.43	26.14	19.30	4.52	11.11	20.58	22.51	0.00	0.00	0.00	0.00
mt	1.86	1.83	1.79	2.28	1.70	1.73	1.73	2.39	2.38	2.29	2.24
il	0.40	0.37	0.33	0.93	0.18	0.21	0.21	1.05	1.05	0.96	0.90
hem	0.00	0.00	0.00	0.00	0.00	0.00	0.00	0.00	0.00	0.00	0.00
ap	0.15	0.12	0.16	0.46	0.04	0.04	0.04	0.45	0.45	0.25	0.25
Rb (ppm)	7.60	4.80	7.60	5.70	4.00	6.00	5.70	19.10	19.50		9.10
Sr	195.90	195.50	328.00	220.00	385.00	370.00	360.00	362.00	354.00		257.00
Ba	110.00	84.80	126.00	134.00	45.50	54.60	55.40	295.00	259.00		241.00
Co	74.40	62.30	59.50	24.40	39.60	44.90	48.40	32.40	29.60		37.00
Cu	22.90	14.00	10.00	<5	<5	<5	<5	26.50	14.00		4.00
Cr	1817.00	1350.00	1440.00	170.00	280.00	360.00	360.00	150.00	90.00		530.00
Ni	365.20	353.00	420.00	57.00	68.00	68.00	70.00	11.20	10.00		114.00
V	216.00	139.00	97.00	258.00	116.00	116.00	117.00	334.00	229.00		179.00
Zn	92.40	80.00	62.00	144.00	42.00	47.00	52.00	110.00	101.00		98.00
Zr	20.80	18.00	19.00	46.00	4.00	6.00	6.00	73.71	65.00		65.00
Y	12.60	5.20	4.50	11.10	1.80	2.10	2.10	17.80	16.10		15.10
Nb		0.60	0.80	2.30	0.20	0.20	0.20	7.40	3.50		3.00
Th	3.50	0.73	0.67	1.80	0.13	0.18	0.20	4.20	2.36		2.12
Ta		0.09	0.10	0.20	<0.1	<0.1	<0.1		0.20		0.20
U		0.20	0.17	0.50	0.05	0.08	0.11		0.59		0.59
Pb	7.90	5.00	4.00	4.00	4.00	4.00	4.00	10.00	21.00		39.00
Hf		0.50	0.50	1.40	<0.2	0.20	0.20		1.90		1.80
La		2.70	2.90	7.10	0.90	1.40	1.60		8.50		8.10
Ce		5.50	5.30	14.30	1.60	2.10	2.40		17.80		16.40
Pr		0.75	0.77	1.94	0.25	0.33	0.36		2.34		2.09
Nd		3.50	3.30	8.20	1.10	1.50	1.60		10.20		9.10
Sm		0.90	0.88	2.04	0.30	0.42	0.41		2.59		2.27
Eu		0.32	0.30	0.66	0.20	0.27	0.28		0.87		0.77
Gd		0.96	0.91	2.17	0.39	0.41	0.41		2.87		2.60
Tb		0.15	0.16	0.37	0.06	0.07	0.08		0.48		0.44
Dy		0.99	0.89	2.09	0.35	0.42	0.41		3.06		2.82
Ho		0.20	0.18	0.46	0.08	0.09	0.08		0.64		0.59
Er		0.63	0.51	1.34	0.22	0.25	0.25		1.89		1.76
Tm		0.09	0.10	0.21	0.06	0.06	0.06		0.26		0.26
Yb		0.56	0.49	1.20	0.19	0.23	0.21		1.83		1.70
Lu		0.08	0.07	0.19	0.03	0.04	0.04		0.27		0.24

continues

Table 3 (continued). Major (wt. %) and trace (ppm) element analyses of the El Fuerte metamorphic rocks.

	Cubampo Granite						Guamuchil Formation				
Sample n°	ELF-200*	ELF-200	ELF-201*	ELF-201	ELF-204*	ELF-204	ELF-207	ELF-208	ELF-209	ELF-210	ELF-211
SiO_2 (wt %)	73.45	74.50	64.17	65.70	76.17	77.60	49.4	52.00	52.30	61.20	51.40
TiO_2	0.16	0.14	0.79	0.73	0.19	0.16	1.02	0.99	0.99	0.46	1.02
Al_2O_3	14.00	13.25	15.50	14.80	11.86	11.20	19.2	18.4	18.15	13.9	18.3
Fe_2O_3	2.15	2.21	7.52	7.16	3.42	3.29	8.87	8.44	9.01	8.47	9.44
MnO	0.02	0.02	0.10	0.10	0.08	0.08	0.16	0.13	0.18	0.07	0.17
MgO	0.43	0.34	1.42	1.37	0.34	0.31	4.41	4.78	5.04	0.06	5.04
CaO	1.40	1.36	3.34	3.19	1.36	1.31	11.95	9.59	11.45	14.25	9.49
Na_2O	3.22	3.77	3.20	3.65	3.62	4.16	2.75	2.96	1.85	0.02	2.77
K_2O	2.65	2.55	2.00	1.87	1.09	1.01	1.07	1.25	0.33	0.01	1.00
P_2O_5	0.03	0.01	0.16	0.13	0.04	0.05	0.31	0.26	0.28	0.14	0.26
LOI	1.38	1.38	1.29	1.29	0.70	0.70	0.89	1.00	0.40	1.10	1.5
Total	98.89	99.53	99.49	99.99	98.86	99.87	100.03	99.80	99.98	99.68	100.39
CIPW											
Q	39.63	37.78	25.65	25.31	45.51	43.77	0.00	2.74	8.35	33.86	2.87
or	16.32	15.56	12.33	11.44	6.73	6.17	6.46	7.51	1.99	0.06	6.04
ab	30.20	34.97	29.99	33.95	33.93	38.52	25.16	27.09	17.05	0.19	25.47
an	7.03	6.90	16.26	15.55	6.76	6.37	37.59	33.92	41.22	40.87	35.33
lc	0.00	0.00	0.00	0.00	0.00	0.00	0.00	0.00	0.00	0.00	0.00
ne	0.00	0.00	0.00	0.00	0.00	0.00	0.00	0.00	0.00	0.00	0.00
C	3.83	2.09	2.70	1.43	2.69	1.12	0.00	0.00	0.00	0.00	0.00
di	0.00	0.00	0.00	0.00	0.00	0.00	16.64	10.35	12.10	15.93	8.92
hy	1.24	0.98	9.08	8.57	2.20	1.94	7.08	13.80	14.63	0.00	16.69
ol	0.00	0.00	0.00	0.00	0.00	0.00	2.29	0.00	0.00	0.00	0.00
mt	0.86	1.04	2.48	2.40	1.81	1.78	2.68	2.64	2.66	2.20	2.68
il	0.23	0.20	1.16	1.06	0.27	0.23	1.45	1.41	1.41	0.70	1.45
hem	0.61	0.47	0.00	0.00	0.00	0.00	0.00	0.00	0.00	0.00	0.00
ap	0.06	0.02	0.34	0.28	0.09	0.11	0.66	0.55	0.60	0.31	0.55
Rb (ppm)	68.10	52.80	82.30	83.50	33.10	24.80	24.90	42.80	9.20	1.00	29.50
Sr	167.7	120.5	178.4	151.5	163.5	118.5	354.00	402.00	330.00	397.00	313.00
Ba	1700	1375	1670	1445	998.0	843.0	492.00	358.00	180.00	14.00	481.00
Co	2.60	1.60	10.00	7.20	5.90	1.60	24.70	22.50	25.80	10.40	26.20
Cu	45.80	17.00	21.90	7.00	59.40	27.00	16.00	24.00	55.00	262.00	39.00
Cr	27.70	9.00	22.80	9.00	42.80	10.00	130.00	100.00	110.00	50.00	110.00
Ni	7.75	4.00	5.57	4.00	8.44	4.00	48.00	29.00	33.00	4.00	25.00
V	14.00	8.00	131.0	65.00	10.00	4.00	183.00	195.00	198.00	183.00	190.00
Zn	48.10	25.00	104.0	81.00	89.60	52.00	79.00	75.00	87.00	11.00	84.00
Zr	174.1.10	110.00	203.90	172.00	283.50	182.00	66.00	71.00	65.00	31.00	71.00
Y	48.00	42.60	40.70	40.70	54.24	59.20	16.30	16.10	16.00	9.10	16.20
Nb	23.20	5.50	21.90	8.20	25.50	6.30	3.70	3.70	3.60	1.60	3.70
Th	16.00	10.60	8.30	7.01	11.00	5.67	1.86	2.18	1.79	0.84	2.24
Ta		0.50		0.60		0.40	0.20	0.20	0.20	0.10	0.20
U		1.81		1.49		1.22	0.54	0.62	0.51	0.48	0.64
Pb	10.00	24.00	7.50	12.00	11.00	11.00	30.00	24.00	13.00	11.00	8.00
Hf		4.00		5.10		5.40	1.80	2.00	1.80	0.80	2.10
La		29.90		21.80		19.60	8.30	9.20	8.20	4.20	9.40
Ce		58.80		45.10		40.10	17.70	19.20	17.10	8.70	19.90
Pr		7.11		5.96		5.24	2.43	2.57	2.32	1.16	2.59
Nd		27.40		24.90		23.00	11.30	11.80	10.60	5.20	11.80
Sm		5.94		5.92		5.94	2.78	2.75	2.69	1.32	2.88
Eu		0.81		1.17		1.15	1.06	1.11	1.01	1.10	1.12
Gd		6.47		6.63		7.16	3.06	3.19	2.99	1.52	3.23
Tb		1.12		1.15		1.35	0.51	0.51	0.49	0.26	0.53
Dy		7.32		7.14		9.35	3.27	3.16	3.11	1.68	3.25
Ho		1.58		1.54		2.15	0.64	0.64	0.63	0.36	0.67
Er		4.95		4.66		6.78	1.88	1.86	1.87	1.09	1.94
Tm		0.72		0.71		1.05	0.27	0.28	0.27	0.16	0.27
Yb		4.79		4.73		7.03	1.78	1.74	1.71	1.09	1.82
Lu		0.74		0.69		1.12	0.26	0.26	0.25	0.16	0.27

continues

Table 3 (continued). Major (wt. %) and trace (ppm) element analyses of the El Fuerte metamorphic rocks.

	Guamuchil Formation									
Sample n°	ELF-214	ELF-216*	ELF-216	ELF-217*	ELF-217	ELF-218	ELF-219*	ELF-219	ELF-220*	ELF-220
SiO_2 (wt %)	63.9	50.54	52.10	57.04	58.90	53.00	36.94	38.10	51.14	51.70
TiO_2	0.66	0.85	0.82	1.49	1.41	0.85	1.03	0.99	0.71	0.65
Al_2O_3	15.35	20.37	20.20	14.96	14.45	14.75	19.16	19.10	14.98	14.30
Fe_2O_3	5.5	9.69	9.26	12.27	12.05	8.58	12.65	12.20	9.49	8.99
MnO	0.11	0.12	0.12	0.23	0.22	0.15	0.19	0.20	0.14	0.14
MgO	1.01	3.95	3.88	2.89	2.80	7.99	12.07	12.00	8.43	8.19
CaO	1.79	10.15	9.38	8.04	7.47	10.15	12.45	11.40	8.86	8.13
Na_2O	4.85	2.12	2.61	1.74	2.25	2.59	0.93	1.35	2.44	2.89
K_2O	3.08	0.11	0.05	0.12	0.06	0.21	0.52	0.44	1.36	1.23
P_2O_5	0.22	0.08	0.12	0.36	0.38	0.29	0.29	0.24	0.20	0.22
LOI	3.18	0.60	0.60	-0.10	-0.10	0.79	3.20	3.20	1.59	1.59
Total	99.65	98.58	99.14	99.03	99.89	99.35	99.43	99.22	99.33	98.03
CIPW										
Q	17.18	6.89	7.51	21.65	22.03	5.15	0.00	0.00	0.12	0.72
or	18.97	0.66	0.30	0.74	0.37	1.25	0.00	0.00	8.24	7.51
ab	45.37	19.80	24.20	16.50	21.16	23.69	0.00	0.00	22.44	26.86
an	7.73	47.67	44.62	34.60	30.50	28.58	48.39	46.42	26.60	23.26
lc	0.00	0.00	0.00	0.00	0.00	0.00	2.55	2.17	0.00	0.00
ne	0.00	0.00	0.00	0.00	0.00	0.00	5.18	7.52	0.00	0.00
C	1.49	0.00	0.00	0.00	0.00	0.00	0.00	0.00	0.00	0.00
di	0.00	3.43	2.06	4.16	4.53	16.69	0.88	7.92	13.73	13.64
hy	5.53	17.62	17.40	16.07	15.33	20.34	0.00	0.00	25.10	24.33
ol	0.00	0.00	0.00	0.00	0.00	0.00	34.38	31.18	0.00	0.00
mt	2.29	2.53	2.48	3.29	3.19	2.48	2.69	2.64	2.33	2.27
il	0.95	1.24	1.18	2.19	2.06	1.21	1.49	1.43	1.01	0.93
hem	0.00	0.00	0.00	0.00	0.00	0.00	0.00	0.00	0.00	0.00
ap	0.48	0.17	0.26	0.79	0.83	0.61	0.63	0.52	0.42	0.48
Rb (ppm)	125.50		0.90		1.40	6.90	9.50	6.40	42.30	45.00
Sr	232.00	219.10	248.00	505.00	516.00	386.00	193.40	186.50	356.00	320.00
Ba	1220.00	110.00	118.00		36.80	241.00	263.00	241.00	346.00	307.00
Co	7.00	20.00	21.20	24.00	19.60	39.30	53.50	43.70	41.40	35.00
Cu	4.00	28.20	23.00	34.00	24.00	90.00	79.00	64.00	11.40	4.00
Cr	9.00	30.00	10.00	46.90	10.00	600.00	1003.00	640.00	433.00	310.00
Ni	4.00	4.43	4.00	2.56	4.00	186.00	193.00	188.00	75.10	70.00
V	39.00	250.00	301.00	357.00	191.00	240.00	408.00	220.00	299.00	192.00
Zn	119.00	84.30	93.00	135.00	128.00	76.00	342.40	304.00	93.00	75.00
Zr	179.00	56.29	67.00	94.06	82.00	41.00	61.60	54.00	73.75	59.00
Y	24.80	14.00	16.60	18.50	23.60	12.20	18.10	15.30	20.10	14.80
Nb	8.00	4.60	3.10	8.80	4.60	2.60	7.00	3.10	6.00	2.80
Th	7.90	2.90	1.00	5.90	3.64	1.42	4.60	1.76	3.80	2.24
Ta	0.50		0.20		0.30	0.10		0.20		0.20
U	2.12		0.24		0.88	0.43		0.48		0.48
Pb	16.00	8.30	13.00	11.00	18.00	15.00	0.00	10.00	8.00	6.00
Hf	5.00		1.90		2.60	1.20		1.60		1.80
La	20.30		7.30		12.30	6.40		7.60		8.20
Ce	38.10		15.70		26.10	13.40		16.00		16.50
Pr	4.83		2.07		3.38	1.82		2.17		2.18
Nd	19.90		9.50		15.10	8.30		10.00		9.60
Sm	4.28		2.28		3.79	2.12		2.58		2.44
Eu	1.11		0.87		1.30	0.81		0.83		0.80
Gd	4.64		2.79		4.32	2.30		2.89		2.76
Tb	0.76		0.48		0.71	0.37		0.48		0.44
Dy	4.69		3.04		4.57	2.37		3.02		2.84
Ho	0.97		0.66		0.97	0.48		0.64		0.57
Er	3.00		2.03		2.87	1.42		1.80		1.73
Tm	0.44		0.28		0.41	0.19		0.26		0.23
Yb	3.06		1.91		2.71	1.29		1.68		1.63
Lu	0.45		0.29		0.40	0.19		0.23		0.23

(*) XRF Laboratory at Universidad de Sonora.

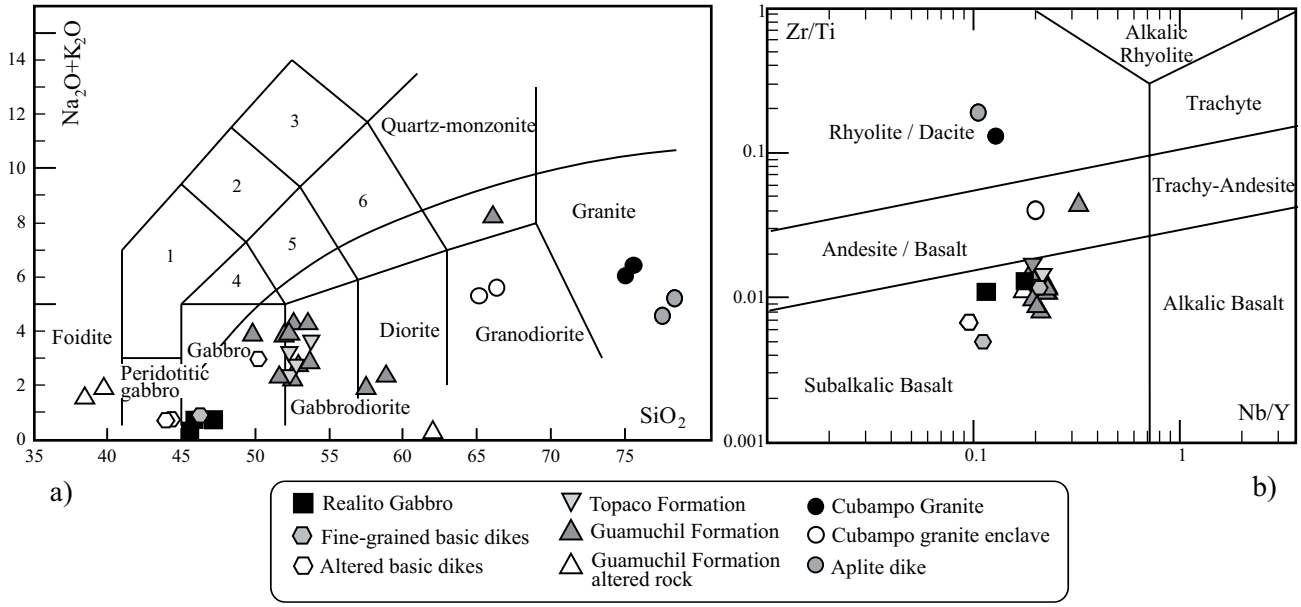

Figure 6. a) Total alkalis *vs*. SiO_2 diagram of the El Fuerte Region rocks (after Middlemost, 1994). Numbered fields: 1, foid–gabbro; 2, foid–monzodiorite; 3, foid–monzosyenite; 4, Monzo-gabbro; 5, Monzo-diorite; 6, Monzonite. Line separating alkaline and subalkaline fields after Miyashiro (1978). b) Zr/Ti *vs* Nb/Y discrimination diagram (after Winchester and Floyd, 1977; Pearce, 1996).

after crustal heating by mafic magmas.

Upper Cretaceous lava flows of the Guamuchil Formation include basaltic andesites, minor basalt, and andesite, all of which have a subalkaline composition (Figure 6a and 6b). These rocks show considerable variation in chemical composition, exemplified by the SiO_2 content from 45 to 66 wt.% (on a volatile free basis). Silica content under 45 wt.% may imply a process of alkaline-basic metasomatism, which cause depletion of acid (SiO_2, F, Cl, SO_3, CO_2, etc.) and input of alkaline/basic (K_2O, Na_2O, CaO, MgO, etc.) components (Zharikov *et al.,* 2007). Samples with low silica of the Guamuchil Formation have higher Ti values than those of the Realito and Topaco formations (0.8 – 1.4 wt.%). Basalt and basaltic andesite are alumina rich (14 – 19 wt. %), with tholeiitic character, which is evidenced by a Fenner trend (Fenner, 1937) in the Al_2O_3-FeO-MgO (AFM) diagram (Figure 7b). REE and multi-elements patterns of the Guamuchil Formation (Figure 8c and 8f) are indistinguishable of those of the Topaco Formation (Figure 8b and 8e), and both units have the same normative minerals including Qtz, Cpx, Opx and Pl, indicating they are quartz tholeiites (Yoder and Tilley, 1962).

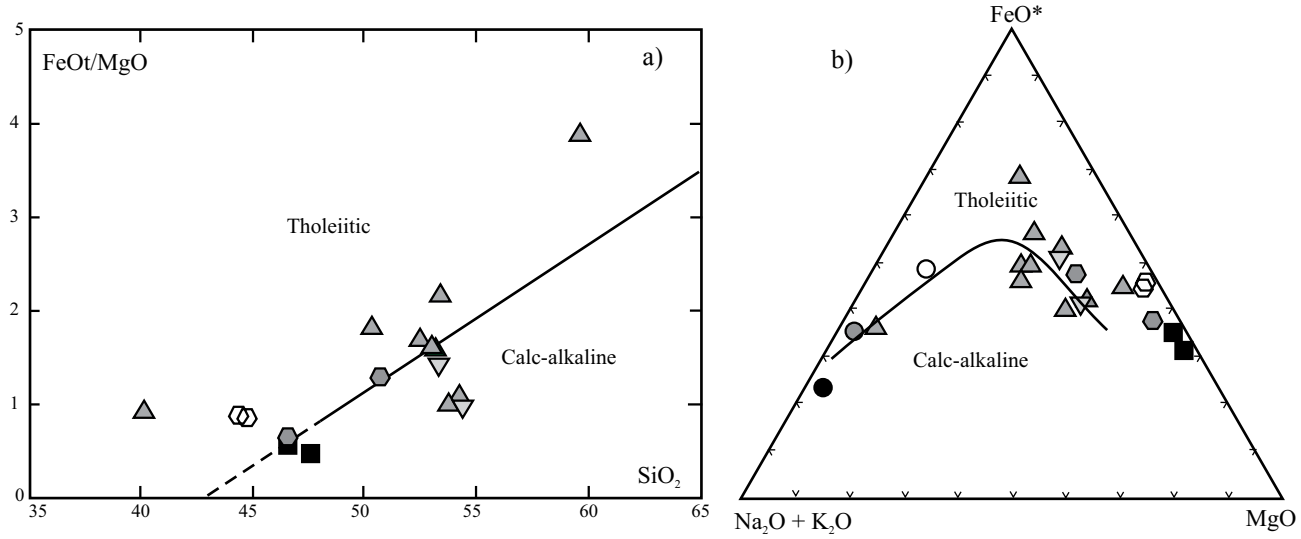

Figure 7. Plotting of the El Fuerte rocks in: a) FeO_t/MgO *vs*. SiO_2 discrimination diagram (after Miyashiro, 1974); b) AFM discrimination diagram, dividing line for tholeiitic and calc-alkaline trends after Irvine and Baragar (1971). Symbols as figure 6.

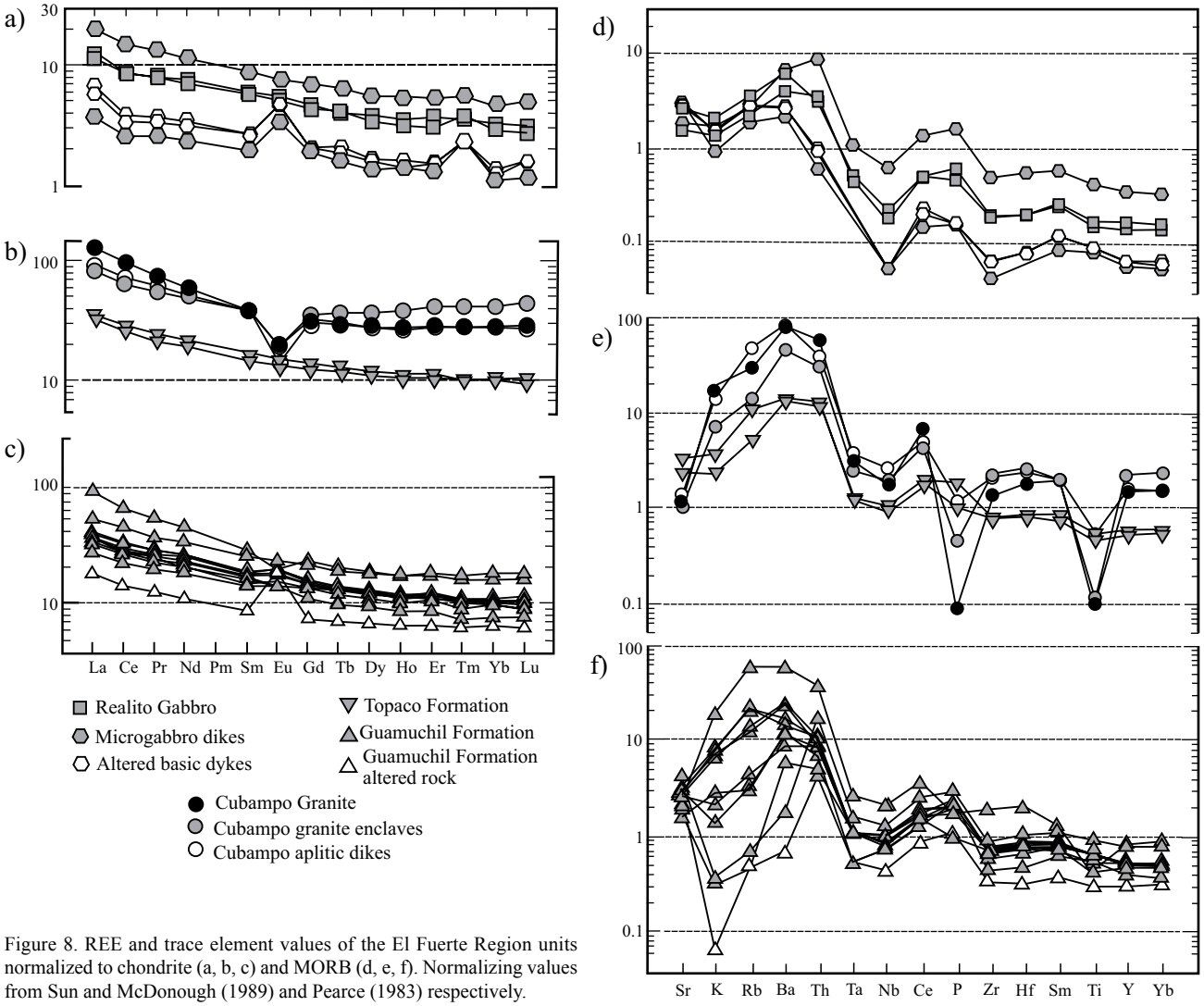

Figure 8. REE and trace element values of the El Fuerte Region units normalized to chondrite (a, b, c) and MORB (d, e, f). Normalizing values from Sun and McDonough (1989) and Pearce (1983) respectively.

Metamorphism

Metamorphism has affected the primary concentrations of SiO_2 and some trace elements in some rocks of the Realito Gabbro, as indicated by higher loss on ignition (LOI) (*e.g.* ELF 226B and ELF 226C) and changes in REE patterns (Figure 8). Altered dikes have higher depletion in most REE excepting La, Eu, and Tm.

In few samples of the Guamuchil Formation, hydrothermal metamorphism replaced original minerals by epidote, actinolite-tremolite, and chlorite. This process is responsible for variation in concentrations of major elements. For example, metasomatic SiO_2 loss in sample ELF 219 originated its plotting in the ultramafic field (Figure 6a), and a sodic alkaline character marked by the presence of leucite and nepheline in the CIPW norm. In spite of variation in major elements of samples ELF 219 and ELF 217 (Figure 6a), ratios of immobile HFS elements (Nb/Y *vs*. Zr/Ti, Figure 6b) and the REE patterns (Figure 8c) are identical to those of other samples in this formation (Figure 8a and 8b); while the multi-element patterns display lower content of K, Rb, and Ba, in the altered samples (Figure 8f). Only the ELF 214 sample displays a differentiated composition with more enriched LREE concentration and subtly negative anomaly in Eu (white triangle in Figure 8c).

Tectonic setting

In order to elucidate the tectonic setting that the El Fuerte samples are more akin, a comparison between analyzed multi-element spectra of the El Fuerte units and those of basalts in present tectonic environments was carry out using the diagram of Pearce (1983) modified by Wilson (1989) (Figure 9a). In this diagram, signatures of the El Fuerte basalts are analogous to those of oceanic island arc environments, with the Guamuchil Formation spectra more similar to oceanic island arc calc-alkaline

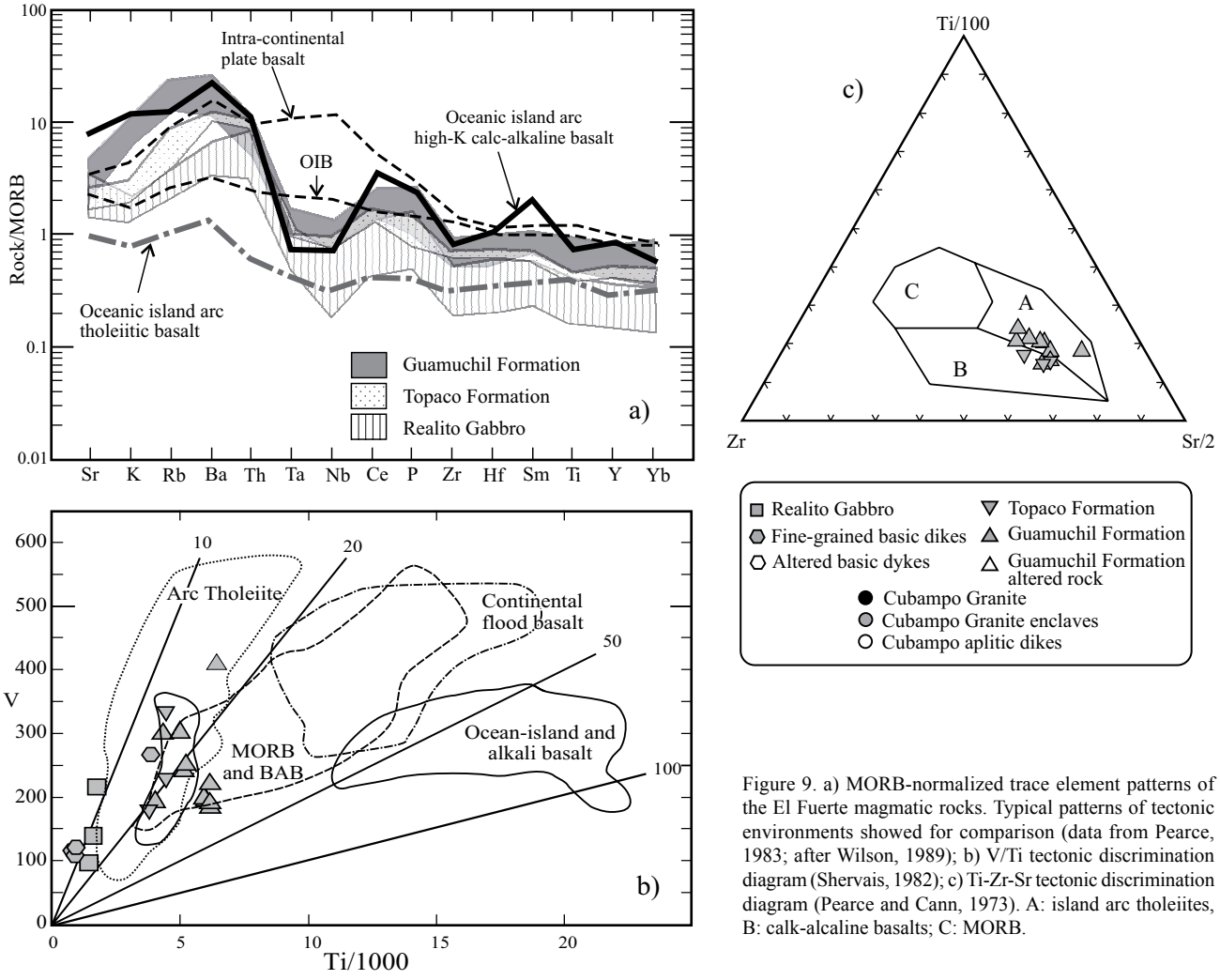

Figure 9. a) MORB-normalized trace element patterns of the El Fuerte magmatic rocks. Typical patterns of tectonic environments showed for comparison (data from Pearce, 1983; after Wilson, 1989); b) V/Ti tectonic discrimination diagram (Shervais, 1982); c) Ti-Zr-Sr tectonic discrimination diagram (Pearce and Cann, 1973). A: island arc tholeiites, B: calk-alcaline basalts; C: MORB.

basalts and those of the Realito Gabbro with a trend to oceanic island-arc tholeiitic basalts. In addition, samples were plotted in the Ti-V diagram of Shervais (1982), which is adequate because these elements are immobile under conditions of hydrothermal alteration and at intermediate-to-high grades of metamorphism (Rollinson, 1993). In the Ti-V diagram, rocks of the Realito Gabbro and Topaco Formation clearly fall in the field of arc tholeiite (Figure 9b). The Guamuchil Formation samples fall in either the arc tholeiite, calc-alkaline, or mid-ocean ridge basalts (MORB) and back-arc basin (BAB) fields. In order to discriminate between the overlapping fields of the Ti-V diagram for the Guamuchil Formation, we use the Ti-Zr-Sr/2 diagram of Pearce and Cann (1973). In this diagram, basalts of the Guamuchil Formation fall in the island-arc tholeiite field (Figure 9c) far from the MORB field. Although Rollinson (1993) indicates that the Ti-Zr-Sr/2 diagram can only be used for fresh samples because of the relative mobility of Sr, the coherent behavior of this element in all samples suggests that no major alteration-related dispersion has occurred.

DISCUSSION

Regional Comparisons

Lower Silurian Realito Gabbro

Silurian magmatic rocks are scarce in Mexico. In our knowledge, only the Acatlán Complex basement of the Mixteco terrane in southern Mexico includes rocks of this age (location in Figure 10). There, batholitic granite with 440–442 Ma U-Pb zircon ages (Ortega-Gutiérrez *et al.*, 1999; Talavera-Mendoza *et al.*, 2005; Vega-Granillo *et al.*, 2007) intrudes into sedimentary rocks and, in turn, basaltic dikes crosscut both types of rock. Subsequently, all of these rocks, grouped as the Esperanza suite, underwent eclogitic metamorphism (Vega-Granillo *et al.*, 2007). However, some unmetamorphosed granites of the Acatlán Complex, also regarded as the Esperanza Granitoids, yield Late Ordovician ages (*e.g.*, Keppie *et al.*, 2008). The age of the eclogitic metamorphism is either Lower Silurian (430 ± 10 Ma, $^{39}Ar/^{40}Ar$ isochron) obtained dating amphibole in eclogite (Vega-Granillo *et al.*, 2007), or Late

Devonian-Mississippian (*e.g.*, Elías-Herrera *et al.*, 2004; Murphy *et al.*, 2006). Esperanza meta-granitoids are peraluminous with calkalcaline continental arc signature (Ramírez-Espinosa, 2001), while the mafic rocks have characteristics of within-plate continental tholeiites (Murphy *et al.*, 2006). In a wider context, Silurian magmatism occurs in the Maya mountains of Belize (Martens *et al.*, 2010), the Appalachian chain (*e.g.*, Whalen *et al.*, 2006), and northwestern South America (Chew *et al.*, 2007). For example, Silurian plutonic suites in the Newfoundland Appalachians include abundant gabbro, monzogabbro and granite to granodiorite and lesser quartz-diorite and tonalite. Mafic rocks include both arc-like (Nb/Th<3) calc-alkaline, and non-arc-like (Nb/Th>3) transitional calc-alkaline basalt to continental tholeiitic affinity compositions (Lissenberg *et al.*, 2006; Whalen *et al.*, 2006). Gabbro complexes have ages from 435 ± 1 to 430 ± 2 Ma (Lissenberg *et al.*, 2006; Whalen *et al.*, 2006). In the Eastern Cordilleras of Perú and Ecuador, subduction-related magmatic rocks yielded ages of 474 to 442 Ma (Chew *et al.*, 2007), but its geochemical character is unknown.

In order to review the probable relation between the Acatlán complex, the Río Fuerte Formation and the Granjeno Schist from southern, northwestern and northeastern Mexico respectively, detrital zircon plots from metamorphic units of each region (data from Talavera-Mendoza *et al.,* 2005; Vega-Granillo *et al.,* 2008; Barboza-Gudiño *et al.,* 2011) were tested through the similarity-overlap method described by Gehrels (2000). Degree of overlap is the degree to which the two age probabilities overlap; there, 1.0 is a perfect overlap, 0.0 indicates no overlap occurs. Degree of similarity is a measure of whether proportions of overlapping ages are similar. Higher values (up to 1.0) reflect similar proportions of overlapping ages. Lower values (down to 0.0) reflect different proportions of ages that may or may not overlap. Results of that comparison, displayed in Table 4, indicate the El Fuerte detrital zircon plots have larger overlap and similarity with those of the Cosoltepec and Ixcamilpa formations of the Acatlán Complex, being both noteworthy high (overlap from 0.74 to 0.81 and similarity from 0.67 to 0.78). However, the Middle to Late Ordovician age of the Río Fuerte Formation precludes correlation with the Cosoltepec Formation because this later unit is considered Early Devonian or younger in age (*e.g.*, Talavera-Mendoza *et al.,* 2005). Besides, the Río Fuerte detrital zircon plots are comparable with those obtained in the Granjeno Schist from Tamaulipas and Nuevo León, Mexico (Barboza-Gudiño *et al.*, 2011) with overlap from 0.86 to 0.77 and similarity between 0.74 and 0.55 (Table 4). In the Table 4, it is also noteworthy the high similarity between some units of the Granjeno Schist with some units in the Acatlán Complex.

Upper Jurassic Cubampo Granite and Topaco Formation

The Late Jurassic ages of the Cubampo Granite and related dikes (Vega-Granillo *et al.*, 2008; 2011) are coeval within analytical errors with the age obtained from the metabasite of the Topaco Formation. Similarities in REE and trace elements concentrations between these two types of rocks, also suggest they are genetically related.

At regional scale, Jurassic magmatic rocks occur in two areas: 1) southwestern Arizona, southeastern California and northwestern Sonora (Tosdal *et al.*, 1989); and 2) Central Mexico (Figure 10). Both areas have been considered as parts of a continuous Late Triassic–Middle Jurassic magmatic arc (Bartolini *et al.*, 2003), or as parts of a truncated arc displaced about 800 to 1000 km to southeast by the Mojave-Sonora megashear (*e.g.*, Anderson *et al.*, 2005; Haxel *et al.*, 2005). In the northwestern area (1),

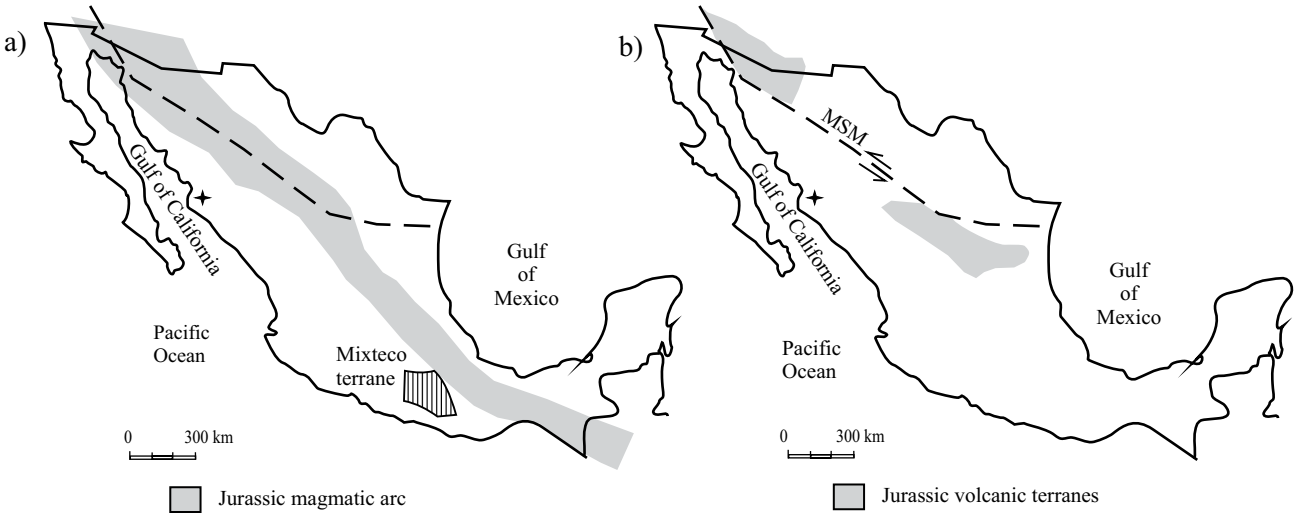

Figure 10. Present distribution of Jurassic magmatism according to: a) Bartolini *et al.* (2003); and b) Jones *et al.* (1995). MSM: Mojave-Sonora megashear; star: study area.

Table 4. Degree of overlap and similarity between the Río Fuerte and Acatlán Complex detrital zircon plots

El Fuerte		Acatlán Complex							Granjeno Schist		
1					**OVERLAP**						
0.882	**2**										
0.609	0.582	**3**									
0.711	0.687	0.650	**4**								
0.778	0.752	0.667	0.819								
0.807	0.811	0.657	0.627	0.722	6						
0.712	0.747	0.741	0.719	0.834	0.801	5					
0.581	0.565	0.766	0.614	0.662	0.683	0.775	**8**				
0.623	0.628	0.751	0.729	0.794	0.707	0.599	0.768	**9**			
0.774	0.796	0.652	0.667	0.699	0.704	0.697	0.668	0.727	**10**		
0.860	0.836	0.615	0.668	0.731	0.715	0.725	0.570	0.587	0.762	**11**	
0.797	0.809	0.765	0.804	0.830	0.744	0.814	0.667	0.722	0.747	0.750	**12**
1					**SIMILARITY**						
0.826	**2**										
0.512	0.591	**3**									
0.677	0.726	0.537	**4**								
0.781	0.765	0.466	0.717	**4**							
0.769	0.727	0.341	0.620	0.816	**6**						
0.611	0.660	0.744	0.592	0.618	0.568	**7**					
0.559	0.575	0.735	0.563	0.582	0.489	0.785	**8**				
0.619	0.679	0.514	0.661	0.725	0.695	0.592	0.522	**9**			
0.709	0.693	0.652	0.667	0.669	0.704	0.697	0.668	0.727	**10**		
0.739	0.650	0.615	0.668	0.731	0.715	0.725	0.570	0.587	0.728	**11**	
0.629	0.552	0.862	0.588	0.467	0.392	0.688	0.595	0.511	0.812	0.734	**12**

1 and 2, samples ELF-24, ELF-07, Río Fuerte Formation (Vega-Granillo *et al.*, 2008); 3 to 9, samples from the Acatlán Complex: 3: Xayacatlán Fm.; 4: Ixcamilpa Formation; 5 and 6: Cosoltepec Fm; 7-8: Chazumba Fm.; 9: Esperanza Fm. (Talavera-Mendoza *et al.*, 2005); 10-12, Granjeno Schist: Arramberi, Miquihuana, Cañon de Caballeros localities (Barboza-Gudiño *et al.*, 2011).

calk-alcaline magmatic rocks yielding ages between 175 and 165 Ma are interpreted as continental arc magmatism (Anderson *et al.*, 2005; Haxel *et al.*, 2005). In the central Mexico area (2), the Nazas Formation is a thick sequence of andesite and dacite with minor rhyolite and latite, capped by red beds (Blickwede, 2001). Welded eutaxitic tuffs in the upper part of the Nazas Formation have U-Pb ages of 172 and 169 Ma (Lawton, 2010). Consequently, the suites from the northwestern and central areas are older than the Cubampo and Topaco formations and cannot be correlated with them.

A regional suite of Upper Jurassic sedimentary, volcanic, and plutonic units, overlies or intrudes Middle Jurassic sequences in southwestern USA (*e.g.*, Saleeby and Busby-Spera, 1992; Anderson *et al.*, 2005). These units (*e.g.*, Artesa, Ko Vaya, McCoy Mountains, Glance formations) yield 165 to 145 Ma ages (*e.g.*, Barth *et al.*, 2004; Anderson *et al.*, 2005; Haxel *et al.*, 2005). The Glance Conglomerate of southwestern Arizona contains abundant rhyolitic, dacitic, and andesitic volcanic and volcaniclastic deposits interstratified with boulder breccia-conglomerates (*e.g.*, Busby *et al.*, 2005). Geochemical data suggest these rocks record a variation from continental arc to rift volcanism (Krebs and Ruiz, 1987; Anderson *et al.*, 2005), or continental arc setting only (Busby *et al.*, 2005). Two granodiorites and one metarhyolite from the Caborca terrane yielded 153 Ma, 164 Ma and 141 Ma ages, respectively (Anderson *et al.*, 2005). In addition, ortogneisses in the eastern Peninsular Ranges in Baja California yielded a 162 Ma age (*e.g.* Alsleben *et al.*, 2008). Whereas, in Central Mexico an intrusive related to the Coapas schist yielded a 158 ± 4 Ma age (U-Pb zircon age, Jones *et al.*, 1995). All previous rocks are nearly coeval to the Cubampo and Topaco dated samples.

In addition to the Late Jurassic magmatism mentioned above and considered as formed in continental arc setting, Late Jurassic-Early Cretaceous magmatism occurs in the Guerrero superterrane (Figure 11c), which includes the Alisitos terrane of Baja California. Some authors consider this superterrane as relatively or partially exotic to Precambrian-Paleozoic terranes composed of Laurentian or Gondwanan blocks forming mainland Mexico (*e.g.*, Campa and Coney, 1983; Dickinson and Lawton, 2001). However, there is no consensus about the exotic origin of the Guerrero superterrane. The Arteaga Complex, considered the basement of the Guerrero superterrane (Centeno-García *et al.*, 2003), consists of metamorphosed sedimentary, volcanic and intrusive rocks assigned to the Late Triassic-Lower Jurassic (Centeno-García *et al.,* 1993). The Tumbiscatío

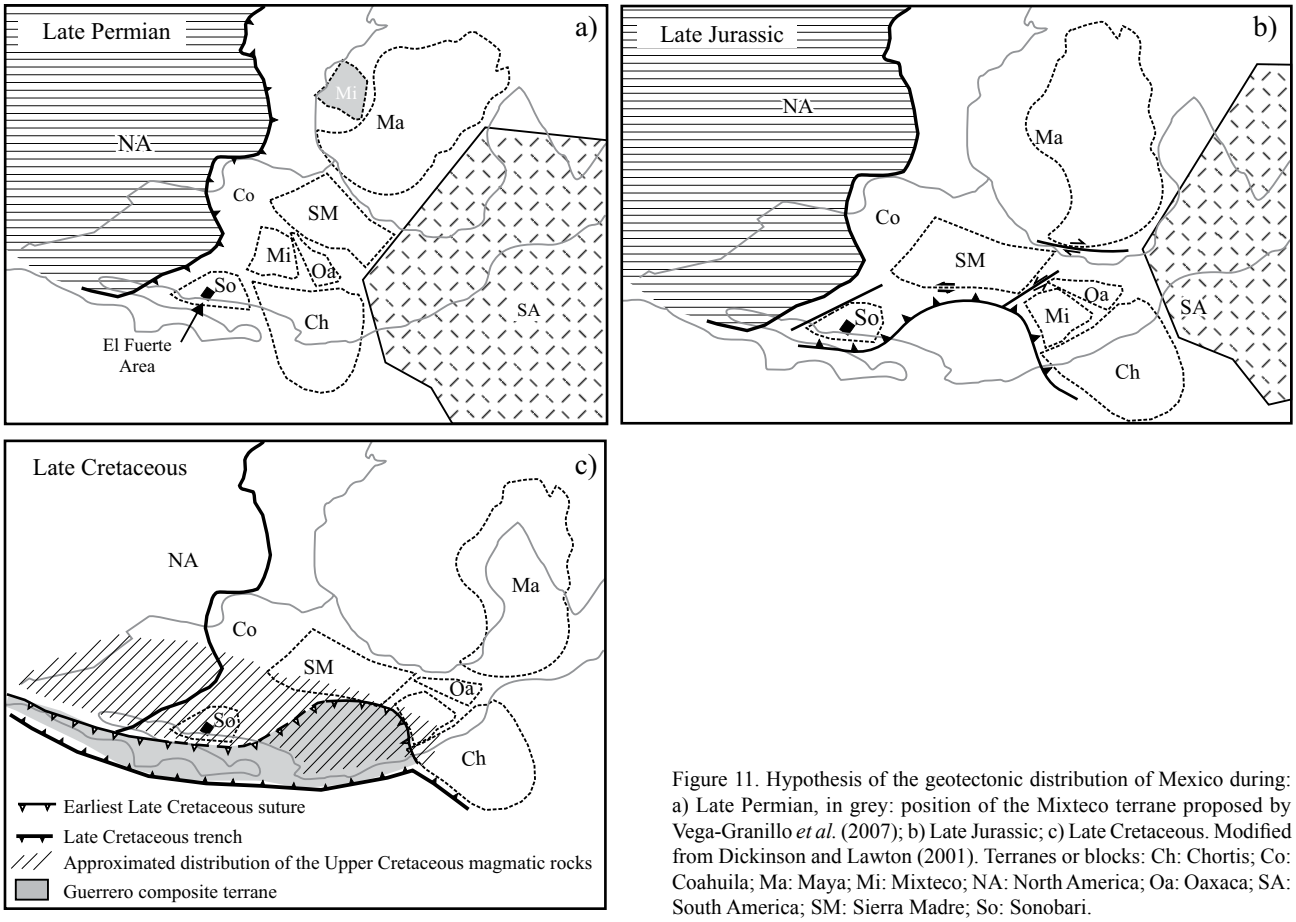

Figure 11. Hypothesis of the geotectonic distribution of Mexico during: a) Late Permian, in grey: position of the Mixteco terrane proposed by Vega-Granillo *et al.* (2007); b) Late Jurassic; c) Late Cretaceous. Modified from Dickinson and Lawton (2001). Terranes or blocks: Ch: Chortis; Co: Coahuila; Ma: Maya; Mi: Mixteco; NA: North America; Oa: Oaxaca; SA: South America; SM: Sierra Madre; So: Sonobari.

Granite intrudes the Arteaga Complex and yielded a U-Pb age of 163 Ma (Centeno-García *et al.*, 2003) and a K-Ar age of 158 ± 5 Ma (Grajales-Nishimura and López-Infanzón, 1984). The arc assemblage of the Guerrero terrane includes basalts yielding K-Ar and $^{39}Ar/^{40}Ar$ ages of 105 to 93 Ma (Delgado-Argote *et al.*, 1990; Ortiz-Hernández and Lapierre, 1991; Elías-Herrera *et al.*, 2000), which are covered by Lower Cretaceous sedimentary rocks (Guerrero-Suástegui *et al.*, 1993; Salinas, 1994). In Guanajuato, a magmatic sequence formed by a cogenetic island-arc tholeiitic suite, ultramafic-mafic cumulate rocks, diabasic feeder dikes, and basaltic pillow lavas (Lapierre *et al.*, 1992) yielded K-Ar ages ranging from 157 to 108 Ma (Ortiz-Hernández *et al.*, 1990; Lapierre *et al.*, 1992). This sequence is thrust to the NNE over a contemporaneous, highly deformed, detrital and volcanic sequence named the Arperos Formation (Monod *et al.*, 1990), which is an island arc tholeiitic suite, ranging from ultramafic-mafic cumulate rocks, diabasic feeder dikes, and basaltic pillow lavas (Lapierre *et al.*, 1992). The lowermost limestone levels of the Arperos Formation contain nannofosils of Tithonian-Hauterivian age (Corona-Chávez, 1988). Limestones with Aptian-Albian fossils (Chiodi *et al.*, 1988; Quintero-Legorreta, 1992) cover the Arperos formation.

In the Vizcaino Peninsula and Cedros Island of western Baja California, magmatism spans from the Late Triassic (221 Ma) to the Early Cretaceous (*ca.* 135 Ma; Kimbrough and Moore, 2003). In that region, the Upper Jurassic-Lower Cretaceous Coloradito and Eugenia Formations contain mudflows and olistostrome blocks interbedded with arc volcanogenic sediment and rift-related pillow lavas. Middle Jurassic to Lower Cretaceous plutonic arc rocks (*ca.* 165–135 Ma) intrude low greenschist facies ophiolite and volcanic arc basement (Kimbrough and Moore, 2003). These intrusions are I-type Cordilleran batholithic rocks, ranging from gabbro to granodiorite, with dominant tonalite, and relatively primitive arc geochemical affinities (initial $^{87}Sr/^{86}Sr$ range from ~0.704 to 0.706), but they are distinctively calcic in nature (Kimbrough and Moore, 2003). A tonalite dated at about 155–152 Ma, a gneissic tonalite of *ca*. 149 Ma, and a leucotonalite containing fractions with ages of 150 to 160 Ma (Kimbrough and Moore, 2003) are coeval to the Cubampo Granite.

Upper Cretaceous Guamuchil Formation

The Upper Cretaceous Guamuchil Formation is coeval with volcanic suites dispersed along the North and South America western border. Late Cretaceous-early Tertiary arc magmatism in east-central Sonora includes the Sonoran batholith and its volcanic equivalent the

Tarahumara Formation (McDowell *et al.*, 2001). The Tarahumara Formation includes about 2500 m of andesitic to dacitic lava, agglomerate, and volcanic breccia, with subordinate felsic pyroclastic components (McDowell *et al.*, 2001), which yielded ages from 90 to 70 Ma (U-Pb zircon; K-Ar biotite and hornblende, *e.g.*, McDowell *et al.*, 2001; Roldán-Quintana, 2002). Rocks ranging in age from 70 to 100 Ma ($^{39}Ar/^{40}Ar$) are common in the Peninsular Ranges province of Baja California (Tulloch and Kimbrough, 2003). In the Sinaloa batholith, which is the southward extension of the Sonora batolith, Henry *et al.* (2003) reported syntectonic intrusions with hornblende K-Ar ages between 98 and 90 Ma; and post-tectonic intrusions emplaced nearly continuous between 90 and 45 Ma.

The Guamuchil Formation cannot be correlated with rocks of the composite Guerrero terrane, because the upper sedimentary part of that terrane has Aptian-Albian fossils (*e.g.*, Allison, 1955; Talavera-Mendoza and Guerrero-Suástegui, 2000) and the lower volcanic part has Lower Cretaceous ages (Delgado-Argote *et al.*, 1990; Ortiz-Hernández and Lapierre, 1991; Elías-Herrera *et al.*, 2000). Furthermore, the Alisitos arc accretion to the continental border occurred before 108 Ma (Wetmore *et al.*, 2002; Alsleben *et al.*, 2008). The Guamuchil Formation may be correlated with the La Unión-Zihuatanejo assemblage occurring in the Zihuatanejo subterrane, which consists of sedimentary rocks interbedded with andesitic lava flows, volcanic breccia, and tuffs. Martini *et al.* (2010) interpreted Late Cretaceous ~88 Ma detrital zircon ages in sedimentary rocks as probably derived from the interbedded tuff units.

Discussion on the tectonic context

In the tectonic model proposed by Vega-Granillo *et al.* (2008), the Río Fuerte Formation deposition occurred in a basin between an active Ordovician arc and an extinct Neoproterozoic peri-Gondwanan arc. Although the Late Ordovician arc was hypothesized on the basis of detrital zircon ages in metasediments of the Río Fuerte Formation, the Realito Gabbro may be the Early Silurian extension of this arc. Geochemical data indicate that the Realito Gabbro emplacement occurred in an island arc tectonic setting. The model of Vega-Granillo *et al.* (2008) proposed south-directed subduction, which eventually may have caused the accretion of the Río Fuerte Formation and the Realito Gabbro to southern Laurentia, probably by Carboniferous–Permian times. The accretion time is constrained by the timing of emplacement of Paleozoic slope and abyssal sequences over coeval platform sequences in Central Sonora (Poole and Madrid, 1988; Poole *et al.*, 2005).

Detrital zircon ages and Silurian magmatism relate the Sonobari Complex of northern Sinaloa with the Acatlán Complex of southern Mexico, suggesting their proximity in Paleozoic times (Figure 11a). However, the geochemical signature, calk-alkaline for the Esperanza Granitoids in the Acatlán Complex and tholeiitic for the Realito Gabbro; and metamorphic conditions, high P/T in the Ixcamilpa and Esperanza suites against low P/T for the Río Fuerte Formation, suggest those regions underwent distinctive tectonic evolutions. Whereas the high P/T metamorphism in the Ixcamilpa suite occurred along a subduction zone (Vega-Granillo *et al.*, 2007), the low P/T metamorphism in the Río Fuerte Formation is more typical of magmatic arc setting (Vega-Granillo *et al.*, 2011).

Considering the present position of the El Fuerte region, the Upper Jurassic felsic-mafic magmatism of that area may have occurred in two scenarios: 1) as a southern prolongation of the Upper Jurassic continental magmatism of northwestern Sonora, eastern Peninsular Ranges and southwestern USA; or 2) as part of the Upper Jurassic-Lower Cretaceous arc assemblages of the Guerrero superterrane (Figure 11b and Figure 12). Considering that the Cubampo Granite and related dikes intrude the Río Fuerte Formation, and clasts of these two units made part of the agglomerates in the Topaco Formation, the Upper Jurassic magmatism must have been emplaced over and/or through the Río Fuerte Formation and the Realito Gabbro. Then, if the accretion of basement sequences to the Laurentian cra-

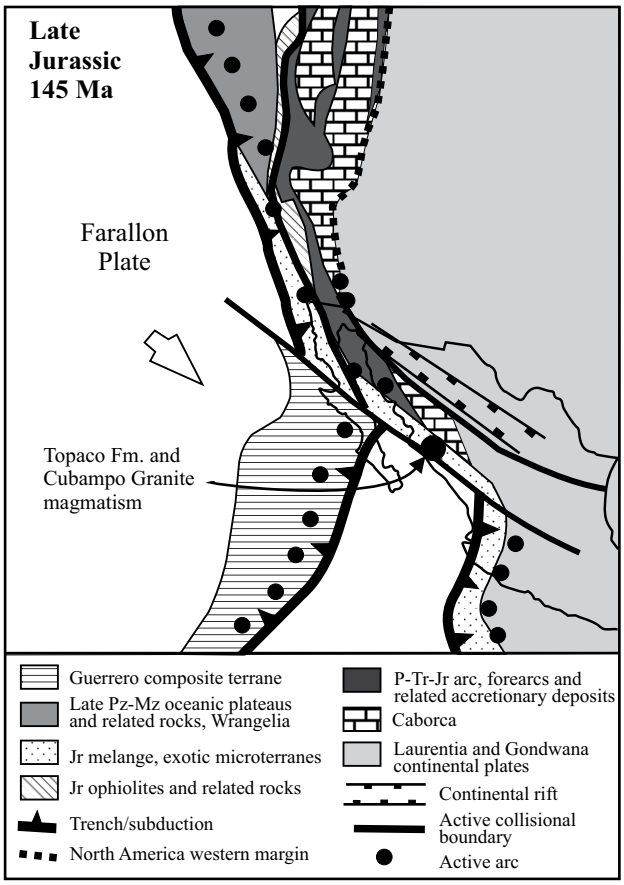

Figure 12. Paleogeographic reconstruction of the Late Jurassic in northwestern Mexico southwestern U.S.A. Modified from Blakey (http://www2.nau.edu/rcb7/jur145seattle.html).

ton occurred since late Paleozoic time, the Upper Jurassic magmatism in the El Fuerte area must be autochthonous. Besides, the Arteaga Complex, basement of the Guerrero terrane, is regarded Late Triassic-Lower Jurassic in age (Centeno-García *et al.*, 1993) and consequently, cannot be correlated with the Middle-Upper Ordovician Río Fuerte Formation. The island arc geochemical character of the Topaco Formation differs from the coeval continental arc magmatism in northern Sonora and southwestern Arizona. Anyway, this variation may be due to differences in the mantle from which these two suites derive, which is supported by Nd and Sr isotopes and REE variations in granites from northern Sonora through northern Sinaloa (Valencia-Moreno *et al.,* 2011).

By Late Cretaceous, the Guerrero superterrane was already accreted to mainland Mexico (*e.g.*, Tardy *et al.*, 1994; Alsleben *et al.*, 2008) (Figure 11c). In this scenario, the Guamuchil Formation may be part of the Late Cretaceous magmatic arc developed along the western border of Mexico, from Sonora to Guerrero (Figure 11c). Again, particular oceanic island-arc signature of the Upper Cretaceous magmatism may derive from the particular mantle source underlying the El Fuerte region.

CONCLUSIONS

In the El Fuerte region northwestern Mexico, four units with igneous rocks crop out:

The Realito Gabbro yielded a 430 ± 15 Ma U-Pb zircon age. This unit intrudes the Middle-Upper Ordovician Río Fuerte Formation, and corresponds to hornblende-pyroxene gabbro with retrogressive metamorphism. Geochemistry studies indicate rocks of this unit are subalkaline island arc tholeiite with komatiitic affinity, which may be caused by cumulate processes.

A Late Jurassic suite made up by the Cubampo Granite and the Topaco Formation. The Cubampo Granite and related aplite dikes with ages between 155 and 151 Ma are peraluminous subalkaline granites. The granite contains quartz-diorite enclaves. The 155 ± 3.5 Ma age yielded by basalts of the Topaco Formation indicates that is coeval with the Cubampo Granite. The Topaco Formation samples correspond to island arc basalts with subalkaline composition and tholeiitic affinity. Similarities in REE and trace elements concentrations between the felsic rocks of the Cubampo Granite and mafic rocks of the Topaco Formation suggest some kind of genetic link between these units, maybe peraluminous granites were formed after crustal heating by mafic magmas.

The Guamuchil Formation mainly consists of basalt and basaltic andesite with subalkaline composition, high alumina but tholeiitic character. A dated sample yielded a 73 ± 1.5 Ma (Campanian) age.

The Early Silurian age of the Realito Gabbro and previously obtained detrital zircon plots of the Río Fuerte Formation (Vega-Granillo *et al.,* 2008), suggests a relationship between the El Fuerte units and the Ixcamilpa and Esperanza suites of the Acatlán Complex of southern Mexico, although subsequently, each region underwent distinctive tectonic evolutions. Petrology and field relationships indicate that the Late Jurassic rocks of the Topaco and Cubampo units were emplaced on or through the Río Fuerte Formation, which was accreted to Laurentia since late Paleozoic time. Consequently, this magmatism is considered authoctonous. The Upper Cretaceous Guamuchil Formation must be part of a large belt of coeval intrusions and volcanic rocks extending from Sonora to Guerrero in Mexico. The island-arc tholeiitic signature of these lavas differs from the continental calc-alkaline character of contemporaneous rocks, and may arise from a distinctive mantle source. At last, regarding the ages obtained from volcanic rocks of the El Fuerte region, the Lower Cretaceous lavas characteristic of the Guerrero terrane were not found in this study.

ACKNOWLEDGEMENTS

The research for this paper was financed by a CONACYT (79759) grant to Ricardo Vega-Granillo. We appreciate helpful assistance of Ken Domanik for microprobe analysis, and Mark Pecha for geochronologic determinations, as well as thoroughly review by Brendan Murphy, Ryan Mathur, and two anonymous reviewers.

REFERENCES

Allison, E.C., 1955, Middle Cretaceous gastropoda of Punta china, Baja California, Mexico: Journal of Paleontology, 29, 400-432.

Alsleben, H., Wetmore, P. H., Schmidt, K. L., Paterson, S. R., Melis, E. A., 2008, Complex deformation during arc-continent collision: Quantifying finite strain in the accreted Alisitos arc, Peninsular Ranges batholith, Baja California: Journal of Structural Geology, 30, 220-236.

Anderson, T.H., Schmidt, V.A., 1983, A model of the evolution of Middle America and the Gulf of Mexico-Caribbean Sea region during Mesozoic time: Geological Society of America Bulletin, 94, 941-966.

Anderson, T.H., Rodríguez-Castañeda, J.L., Silver, L.T., 2005, Jurassic rocks in Sonora, Mexico: Relations to the Mojave-Sonora megashear and its inferred northwestward extension, *in* Anderson, T.H., Nourse, J.A., McKee, J.W., Steiner, M.B. (eds.), The Mojave-Sonora Megashear Hypothesis: Development, assessment, and alternatives: Geological Society of America Special Paper 393, 51-95.

Barboza-Gudiño, J.R., Ramírez-Fernández, J.A., Torres-Sánchez, S.A., Valencia, V.A., 2011, Geocronología de circones detríticos de diferentes localidades del Esquisto Granjeno en el noreste de México: Boletín de la Sociedad Geológica Mexicana, 63(2), 201-216.

Barth, A.P., Wooden, J.L., Jacobson, C.J., Probst, K., 2004, U-Pb geochronology and geochemistry of the McCoy Mountains Formation, southeastern California: A Cretaceous retroarc foreland basin: Geological Society of America Bulletin, 116, 142-153.

Bartolini, C., Lang, H., Spell, T., 2003, Geochronology, geochemistry,

and tectonic setting of the Mesozoic Nazas arc in North-Central Mexico, and its continuation to northern South America, *in* Bartolini, C., Fuffler, R.T., Blickwede, J. (eds.), The Cicum-Gulf of Mexico and the Caribbean: Hydrocarbon habitats, basin formation, and plate tectonics: American Association of Petroleum Geologists, Memoir, 79, 427 – 461.

Best, M., 2003, Igneous and Metamorphic Petrology: Blackwell Science Ltd, (second edition), 729 p.

Blickwede, J.F., 2001, The Nazas Formation: a detailed look at the early Mesozoic convergent margin along the western rim of the Gulf of Mexico Basin, *in* Bartolini, C., Buffler, R.T., Cantú-Chapa, A. (eds.), The western Gulf of Mexico Basin: Tectonics, sedimentary basins, and petroleum systems: American Association of Petroleum Geologists Memoir 75, 317-342.

Busby, C.J., Bassett, K., Steiner, M.B., Riggs, N.R., 2005, Climatic and tectonic controls on Jurassic intra-arc basins related to northward drift of North America, *in* Anderson, T.H., Nourse, J.A., McKee, J.W., Steiner, M.B. (eds.), The Mojave-Sonora Megashear Hypothesis: Development, Assessment, and Alternatives: Geological Society of America, Special Paper 393, 359–376.

Campa, M.F., Coney, P.J., 1983, Tectono-stratigraphic terranes and mineral resource distributions of Mexico: Canadian Journal of Earth Sciences, 20, 1040-1051.

Centeno-García, E., García, J. L., Guerrero-Suástegui, M., Ramíre-Espinosa, J., Salinas-Prieto, J. C., Talavera-Mendoza, O., 1993, Geology of the southern part of the Guerrero Terrane, Ciudad Altamirano-Teloloapan area, *in* Ortega-Gutiérrez, F. (ed.), Proceedings of the first Circum Pacific and Circum-Atlantic Terrane Conference, Guanajuato, Mexico: Universidad Nacional Autónoma de México, Instituto de Geología, 22-33.

Centeno-García, E., Corona-Chavez, P., Talavera-Mendoza, O., Iriondo, A., 2003, Geology and tectonic evolution of the Western Guerrero terrane-A transect from Puerto Vallarta to Zihuatanejo, México, *in* Alcayde, M., Gómez-Caballero, A. (eds.), Geologic Transects across Cordilleran México: Guidebook for Field Trips of the 99th Geological Society of America Cordilleran Section Meeting: Universidad Nacional Autónoma de México, Instituto de Geologia, Publicación Especial no. 1, 201–228.

Chew, D.M., Kosler J., Whitehouse, M.J., Gutjahr, M., Spikings R.A., Miskovic, A., 2007, U-Pb geochronologic evidence for the evolution of the Gondwanan margin of the north-central Andes, Geological Society of America Bulletin, 119 (5-6), 697-711.

Chiodi, M., Monod, O., Busnardo, R., Gaspard, D., Sánchez, A., Yta, M., 1988, Une discordance anté-albienne datée par una faune d'ammonites et de brachiopodes de type téthysien au Mexique central: Geobios, 21, 125-135.

Corona-Chávez, P., 1988, Análisis estratigráfico-estructural de la porción centro-sur de la Sierra de Guanajuato: México, D.F., Instituto Politécnico Nacional, Escuela Superior de Ingeniería y Arquitectura, tesis profesional, 60 pp. (unpublished).

Damon, P.E., Shafiqullah, M., Roldán-Quintana, J., Cochemé, J.J., 1983, El batolito Laramide (90-40 Ma) de Sonora: Guadalajara, Jalisco, Asociación de Ingenieros de Minas, Metalurgistas y Geólogos de México, Memoria Técnica XV, 63-95.

De Cserna, Z., Kent B.H., 1961, Mapa geológico de reconocimiento y secciones estructurales de la región de San Blas y El Fuerte, Estado de Sinaloa: Cartas Geológicas y Mineras No. 4, escala 1:100,000: Universidad Nacional Autónoma de México, Instituto de Geología.

Delgado-Argote, L., López-Martínez, M., York, D., Hall, C.M., 1990, Geology and geochronology of ultramafic localities in the Cuicateco and Tierra Caliente Complexes, southern Mexico: Geological Society of America, Abstracts with programs 22, 326.

Dickinson, W.R., Lawton, T, F., 2001, Carboniferous to Cretaceous assembly and fragmentation of Mexico: Geological Society of America Bulletin, 113(9), 1142–1160.

Elías-Herrera, M., Sánchez-Zavala, J.L., Macías-Romo, C., 2000, Geologic and geocronologic data from Guerrero Terrane in the Tejupilco area, southern México: new constrains on its tectonic interpretation: Journal of South American Earth Sciences, special issue Geologic evolution of the Guerrero Terrane, western Mexico, 13-15, 355-376.

Elías-Herrera, M., Ortega-Gutiérrez, F., Sánchez-Zavala, J.L., Reyes-Salas, A.M., Macías-Romo, C., Iriondo, A., 2004, New geochronological and stratigraphic data related to the Paleozoic evolution of the high-P Piaxtla Group, Acatlán Complex, southern Mexico, *in* Libro de Resúmenes IV Reunion Nacional de Ciencias de la Tierra, Juriquilla, Querétaro, p. 150.

Fenner, C.N., 1937, A view of magmatic differentiation: Journal of Geology, 45, 158–168.

Gehrels, G.E., 2000, Introduction to detrital zircon studies of Paleozoic and Triassic strata in western Nevada and northern California, *in* Soreghan, M.J., Gehrels, G.E. (eds.), Paleozoic and Triassic Paleogeography and Tectonics of Western Nevada and Northern California: Geological Society of America, Special Paper 347, 1-17.

Gehrels, G.E., DeCelles, P.G., Ojha, T.P., Upreti B.N., 2006, Geologic and U-Th-Pb geochronologic evidence for early Paleozoic tectonism in the Kathmandu thrust sheet, central Nepal Himalaya: Geological Society of America Bulletin, 118 (1-2), 185-198.

Grajales-Nishimura, M., López-Infanzón, M., 1984, Estudio petrogénetico de las rocas ígneas y metamórficas en el Prospecto Tomatlán-Guerrero-Jalisco: Instituto Mexicano del Petróleo, Subdirección de Tecnología y Exploración, Proyecto C-1160 (unpublished).

Guerrero-Suástegui, M., Talavera-Mendoza, O., Ramírez-Espinosa, J., Rodríguez, J., 1993, Estratigrafía y características de depósito del conjunto petrotectónico de Teloloapan, Terreno Guerrero, México, *in* Ortega-Gutiérrez, F. (ed.), Proceedings of the First Circum-Pacific and Circum-Atlantic Terrane Conference: Guanajuato, México, 61-63.

Haxel, G.B., Wright, J.E., Riggs, N.R., Tosdal, R.M., May, D.J., 2005, Middle Jurassic Topawa Group, Baboquivari Mountains, south-central Arizona: volcanic and sedimentary record of deep basins within the Jurassic magmatic arc, *in* Anderson, T.H., Nourse, J.A., McKee, J.W., Steiner, M.B. (eds.), The Mojave-Sonora ;Megashear Hypothesis: development, assessment, and alternatives: Geological Society of America Special Paper 393, 329-357.

Henry, C.D., McDowell, F.W., Silver, L.T., 2003, Geology and geochronology of granitic batholitic complex, Sinaloa, México: Implications for Cordilleran magmatism and tectonics, *in* Johnson, S.E., Paterson, S.R., Fletcher, J.M., Girty, G.H., Kimbrough, D.L., Martín-Barajas, A. (eds.), Tectonic Evolution of Northwestern México and the Southwestern USA: Boulder, Colorado, Geological Society of America, Special Paper 374, 237–273.

Irvine, T.N., Baragar, W.R.A., 1971, A guide to the chemical classification of the common volcanic rocks: Canadian Journal of Earth Sciences, 8, 523-548.

Jones, N.W., McKee, J.W., Anderson, T.H., Silver, L.T., 1995, Jurassic volcanic rocks in northern Mexico: A possible remnant of a Cordilleran magmatic arc, *in* Jacques- Ayala, C., and Roldán-Quintana, J. (eds.), Studies on the Mesozoic of Sonora and adjacent areas: Geological Society of America, Special Paper 301, 179–190

Keppie, D.J., Dostal, J., Miller, B.V., Ortega-Rivera, A., Roldán-Quintana, J., Lee, J.W.K., 2006, Geochronology and geochemistry of the Francisco Gneiss: Triassic continental rift tholeiites on the Mexican margin of Pangea metamorphosed and exhumed in a Tertiary core complex: International Geology Review, 48(1), 1-16.

Keppie, J.D., Dostal, J., Miller, B.V., Ramos-Arias, M.A., Morales-Gámez, M., Nance, D.M., Murphy, B., Ortega-Rivera, A., Lee, J.W.K., Housh, T., Cooper, P., 2008, Ordovician–earliest Silurian rift tholeiites in the Acatlán Complex, southern Mexico: Evidence of rifting on the southern margin of the Rheic Ocean: Tectonophysics, 461, 130-156.

Kimbrough, D.L., Moore, T.E., 2003, Ophiolite and volcanic arc assemblages on the Vizcaino Peninsula and Cedros Island, Baja California Sur, Mexico: Mesozoic forearc lithosphere of the Cordilleran magmatic arc, *in* Johnson, S.E., Paterson, S.R., Fletcher, J., Girty, G.H., Kimbrough, D.L., Martin-Barajas,

A. (eds.), Tectonic evolution of northwestern Mexico and the southwestern USA: A Volume in Honor of R. Gordon Gastil: Geological Society of America, Special Paper 374, 43-71.

Krebs, C., Ruiz, J., 1987, Petrology of the Canelo Hill volcanic: Arizona Geology Digest, 18, 139-151.

Lapierre, H., Ortiz, H.E., Abouchami, N.V., Monod, O., Coulon, C., Zimmermann, J.L., 1992, A crustal section of an intra-oceanic island arc: The Late Jurassic-Early Cretaceous Guanajuato magmatic sequence (central Mexico): Earth and Planetary Sciences Letters, 108, 61-67.

Lawton, T., 2010, Latest Triassic-Middle Jurassic age of cordilleran-Nazas arc in Mexico indicated by U-Pb detrital zircon and volcanic-rock ages: Geological Society of America, Abstracts with Programs, 42(5), 345

Leake, B.E. *et al.*, 1997, Nomenclature of amphiboles: report of the subcommittee on amphiboles of the International Mineralogical Association, Commission on new mineral names: The Canadian Mineralogist, 35, 219-246

Lissenberg, C.J., McNicoll, V.J., van Staal, C.R., 2006, The origin of mafic-ultramafic bodies within the northern Dashwoods Subzone, Newfoundland Appalachians: Atlantic Geology, 42, 1-12.

Martens, U., Weber, B., Valencia, V., 2010, U/Pb geochronology of Devonian and older Paleozoic beds in the southeastern Maya block, Central America: Its affinity with peri-Gondwanan terranes: Geological Society of America Bulletin, 122 (5/6), 815-829.

Martini, M., Ferrari, L., López-Martínez, M., 2010, Stratigraphic redefinition of the Zihuatanejo area, southwestern Mexico: Revista Mexicana de Ciencias Geológicas, 27, 412-430.

McDowell, F.W., Roldán-Quintana, J., Connelly, J.N., 2001, Duration of Late Cretaceous–early Tertiary magmatism in east-central Sonora, Mexico: Bulletin of the Geological Society of America, 113, 521–531.

Middlemost, E. A. K., 1994, Naming materials in magma/igneous rock system: Earth Science Reviews, 37, 215–224.

Miyashiro, A., 1974, Volcanic rocks series in island arcs and active continental margins: American Journal of Sciences, 274, 321-355.

Miyashiro, A., 1978, Nature of alkalic volcanic rock series: Contributions to Mineralogy and Petrology, 66, 91-104.

Monod, O., Lapierre, H., Chiodi, M, Martínez R. J., Calvet, P, Ortiz, H.L.E., Zimmermann, J.L., 1990, Reconstitution d´un arc insulaires intra-océanique au Mexique central- la séquence intra-océanique au Mexique central- la sequence volcano-plutoique de Guanajuato (Crétacé inferieur): Comptes Rendus Hebdomadaires des Séances de l´Acadçémie des Sciences (Paris), ser. 2., v. 310, 45-51.

Morimoto, N., Fabries, J., Ferguson, A.K., Ginzburg, I.V., Ross, M., Seifert, F.A., Zussman, J., Aoki, K., Gottardi, D., 1988, Nomenclature of pyroxenes: American Mineralogist, 62, 53-62.

Mullan, H.S., 1978, Evolution of the Nevadan orogen in northwestern Mexico: Geological Society of America Bulletin, 89(8), 1175-1188.

Murphy, J.B., Keppie, J.D., Nance, R.D., Miller, B.V., Dostal, J., Middleton, M., Fernández-Suarez, J., Jeffries, T.E., Storey, C.D., 2006, Geochemistry and U-Pb protolith ages of eclogitic rocks of the Asís Lithodeme, Piaxtla Suite, Acatlán Complex, southern Mexico: tectonothermal activity along the southern margin of the Rheic Ocean: Journal of the Geological Society of London, 163, 683-695.

Ortiz-Hernández, L.E., Lapierre, H., 1991, Las secuencias toleíticas de Guanajuato y Arcelia, México centro-meridional: Remanentes de un arco insular intra-oceánico del Jurásico superior-Cretácico inferior: Zentralblatt für Geologie und Paläntologie, Teil I, 6, 1503-1517.

Ortiz-Hernández, L.E., Chiodi, M., Lapierre, H., Monod, O., Calvet, P., 1990, El arco intraoceánico alóctono (Cretácico Inferior) de Guanajuato –características petrográficas, geoquímicas, estructurales e isotópicas del complejo filoniano y de las lavas basálticas asociadas: implicaciones geodinámicas: Universidad Nacional Autónoma de México, Revista del Instituto de Geología, 9(2), 126-145.

Ortega-Gutiérrez, F., Elías-Herrera. M., Macías-Romero, C., López, R., 1999, Late Ordovician-Early Silurian continental collisional orogeny in southern Mexico and its bearing on Gondwana-Laurentia connections: Geology, 27 (8), 719-722.

Pearce, J.A., 1983, Role of the sub-continental lithosphere in magma genesis at active continental margins, *in* Hawkesworth, C.J., Norry, M.J. (eds.), Continental basalts and mantle xenoliths, Shiva, Nantwich, Cheshire, United Kingdom, 230- 250.

Pearce, J.A., 1996, A user's guide to basalt discrimination diagrams, *in* Wyman, D.A. (ed.), Trace element geochemistry of volcanic rocks: Applications for massive sulphide exploration: Geological Association of Canada, Short Course Notes, 12, 79-113.

Pearce, J.A., Cann, J.R., 1973, Tectonic setting of basic volcanic rocks determined using trace elements analyses: Earth and Planetary Science Letters, 19, 290-300.

Poole, F.G., Madrid, R.J., 1988, Allochtonous Paleozoic eugeoclinal rocks of the Barita de Sonora mine area, central Sonora, Mexico, *in* Rodríguez-Torres, R. (ed.), El Paleozoico de la región central del Estado de Sonora: Libreto Guía de la Excursión para el Segundo Simposio sobre la Geología y Minería en el Estado de Sonora: Universidad Nacional Autónoma de México, Instituto de Geología, 32-41.

Poole, F. G., Perry Jr., W.J., Madrid, R.J., Amaya-Martínez, R., 2005, Tectonic synthesis of the Ouachita-Marathon-Sonora orogenic margin of southern Laurentia: Stratigraphic and structural implications for timing of deformational events and plate-tectonic model, *in* Anderson, T.H., Nourse, J.A., McKee, J.W., Steiner, M.B. (eds.): The Mojave-Sonora Megashear Hypothesis: Development, Assessment, and Alternatives: Geological Society of America, Special Paper 393, 543-596.

Quintero-Legorreta, O., 1992, Geología de la región de Comanja, estados de Guanajuato y Jalisco: Universidad Nacional Autónoma de México, Revista del Instituto de Geología, 10(1), 6-25.

Ramírez-Espinosa, J., 2001, Tectono-magmatic evolution of the Paleozoic Acatlán Complex in southern Mexico, and its correlation with the Appalachian system: Tucson, Arizona, U.S.A., University of Arizona, Ph.D. thesis, 177 pp.

Roldán-Quintana, J., 2002, Caracterización geológico-geoquímica y evolución del arco magmático Mesozoico-Terciario entre San Carlos y Maycoba, sur de Sonora: México, D. F., Universidad Nacional Autónoma de México, tesis doctoral, 185 pp.

Rollinson, H.R., 1993, Using geochemical data: evaluation, presentation, interpretation: Pearson-Prentice Hall, 352 pp.

Rubatto, D., 2002, Zircon trace element geochemistry: partitioning with garnet and the link between U-Pb ages and metamorphism: Chemical Geology 184, 123-138.

Saleeby, J.R., C. Busby-Spera. 1992. Early Mesozoic tectonic evolution of the western U.S. Cordillera, *in* Burchfiel, B.C., Lipman, P.W., Zoback, M.L. (eds.), The Cordilleran Orogen: Conterminous U.S.: Boulder, Geological Society of America, The Geology of North America, G-3, 107-168.

Salinas, J.C. 1994. Etude structurale du Sud-ouest Mexicain (Guerrero): Analyse Microtectonique des Déformations Ductiles dy Tertiaire inferrieur: Orléans, France, Universite d'Orleans, Thèse du doctorat, 230 pp.

Seiferd, K., Gibson, I., Weis, D., Brunotte, D., 1996, Geochemistry of metamorphosed cumulate gabbros from hole 900A, Iberia Abyssal Plain, *in* Withmarsh, R.B., Sawyer, D.S., Klaus, A., Masson, D.G. (eds.): Procceeding of the Ocean Drilling Program, Scientific Results, 149, 471-488.

Shervais, J.W., 1982, Ti-V plots and petrogenesis of modern and ophiolitic lavas: Earth and Planetary Science Letters, 59, 101-118.

Sun, S.S., McDonough W. F., 1989, Chemical and isotopic systematics of oceanic basalts: implications for mantle compositional processes, *in* Saunders A.D., Norry M.J. (eds.), Magmatism in Ocean Basins: Geological Society of London, Special Publication 42, 313-345.

Talavera-Mendoza, O., Guerrero-Suástegui, M., 2000, Geochemistry and isotopic composition of the Guerrero Terrane (western Mexico): implications for the tectono-magmatic evolution of the southwestern North America during the Late Mesozoic: Journal of South American Earth Sciences, 13, 297-324.

Talavera-Mendoza O., Ruiz, J., Gehrels, G.E., Meza-Figueroa, D.M., Vega-Granillo, R., Campa-Uranga, M. F., 2005, U-Pb geochronology of the Acatlán Complex and implications for the Paleozoic paleogeography and tectonic evolution of southern Mexico: Earth and Planetary Sciences Letters, 235, 682-699.

Tardy, M., Lapierre, H., Freydier, C., Coulon, C., Gill, J., Mercier de Lepinay, B., Beck, C., Martínez, J., Talavera Mendoza, O., Ortiz, E., Stein, G., Yta, M., 1994, The Guerrero suspect terrane (western México) and coeval arc terranes (the Greater Antilles and the western Cordillera of Colombie): A late Mesozoic intra-oceanic arc accreted during Late Cretaceous: Tectonophysics, 230, 49-73.

Tosdal, R.M., Haxel, G.B., Wright, J.E., 1989, Jurassic geology of the Sonoran desert region, southern Arizona, southeastern California, and northernmost Sonora-Construction of a continental-margin magmatic arc, *in* Jenny, J.P., Reynolds, S.J. (eds.), Geologic evolution of Arizona: Arizona Geological Society Digest, 17, 297-434.

Tulloch, A.J., Kimbrough, D.L., 2003, Paired plutonic belts in convergent margins and the development of high Sr/Y magmatism: Peninsular Ranges Batholith of Baja California and Median Batholith of New Zealand, *in* Johnson, S.E.; Paterson, S.R., Fletcher, J.M., Girty, G.H., Kimbrough, D.L., Martin-Barajas, A. (eds.), Tectonic Evolution of Northwestern Mexico and the Southwestern U.S.A.: Geological Society of America, Special Paper 374, 275–295.

Valencia-Moreno, M., Ruiz, J., Barton, M.D., Patchett, P.J., Zurcher, L., Hodkinson, D.G., Roldán-Quintana, J., 2011, A chemical and isotopic study of the Laramide granitic belt of Northwestern Mexico: Identification of the southern edge of the North American Precambrian basement: Geological Society of America Bulletin, 113(11), 1409-1422.

Vega-Granillo, R., Talavera Mendoza, O., Meza-Figueroa, D., Ruiz, J., Gehrels, G., López Martínez, M., de la Cruz Vargas, J.C., 2007, Pressure-temperature-time evolution of Paleozoic high-pressure rocks of the Acatlán Complex (southern Mexico): implications for the evolution of the Iapetus and Rheic Oceans: Geological Society of America Bulletin, 119, 1249-1264.

Vega-Granillo, R., Salgado-Souto, S., Herrera-Urbina, S., Valencia, V., Ruiz, J., Meza-Figueroa, D., Talavera-Mendoza, O., 2008, U-Pb detrital zircon data of the Rio Fuerte Formation (NW Mexico): its peri-Gondwanan provenance and exotic nature in relation to southwestern North America: Journal South American Earth Sciences, 26, 343-354.

Vega-Granillo, R., Salgado Souto S., Herrera Urbina S., Valencia Gómez, V., Vidal Solano, J.R., 2011, Metamorphism and deformation in the El Fuerte region: their role in the tectonic evolution of NW Mexico: Revista Mexicana de Ciencias Geológicas, 28(1), 10-23.

Wetmore, P.H., Schmidt, K.L., Paterson, S.R., Herzig, C., 2002, Tectonic implications for the along-strike variation of the Peninsular Ranges Batholith, Southern and Baja California: Geology, 30, 247-250.

Whalen, J.B., McNicolla, V.J., van Staal, C.R., Lissenberg, C.J., Longstafec, F.J., Jenner, G.A., van Bremman, O., 2006, Spatial, temporal and geochemical characteristics of Silurian collision-zone magmatism, Newfoundland Appalachians: An example of a rapidly evolving magmatic system related to slab break-off: Lithos, 89(3-4), 377-404.

Wilson, M., 1989, Igneous Petrogenesis: Dordrecht, Netherlands, Springer, 466 pp.

Winchester, J.A., Floyd, P.A., 1977, Geochemical discrimination of different magma series and their differentiation products using immobile elements: Chemical Geology, 20, 325-342.

Yoder, H.S., Tilley, C.E., 1962, Origin of basalt magmas: an experimental study of natural and synthetic rock systems: Journal of Petrology, 3, 342-532.

Zharikov, V., Pertsev, N., Rusinov, V., Callegari, E., Fettes, D., 2007, Metasomatism and metasomatic rocks, *in* Fettes, D., Desmons, J. (eds.), Metamorphic Rocks -A classification and glossary of terms: Cambridge University Press, 58-68.

Manucript received: November 3, 2011
Corrected manuscript received: April 18, 2012
Manuscript accepted: April 24, 2012